NTNU – Trondheim
Norwegian University of
Science and Technology

Numerical and Experimental Investigation of Parametric Roll

Johannes Joachim Kalevi
Geyssel

Marine Technology
Submission date: June 2013
Supervisor: Marilena Greco, IMT

Norwegian University of Science and Technology
Department of Marine Technology

NTNU

Norwegian University of
Science and Technology

MASTER THESIS

Numerical and Experimental Investigation of Parametric Roll

Author:
Johannes Geyssel

Supervisor:
Prof. Marilena Greco

June 8, 2013

NTNU Trondheim
Norwegian University of Science and Technology
Faculty of Engineering Science and Technology
Department of MarineTechnology

MASTER THESIS IN MARINE TECHNOLOGY

SPRING 2013

FOR

Johannes Geyssel

Numerical and Experimental Investigation of Parametric Roll

(Numerisk og eksperimentell undersøkelse av Parametric Roll)

Parametric roll is a phenomenon relevant both for large and small vehicles, e.g. for cruise vessels as well as for fishing vessels, advancing in waves. It is both an instability and a resonance phenomenon. It may lead to a significant amplification of the roll motion, oscillating at the natural frequency, and is connected with the periodic change, with the excitation period, of the restoring arm as the ship moves in waves. Its occurrence requires a certain link between the roll natural frequency and the excitation frequency and implies that the damping of the ship to dissipate the parametric roll energy is insufficient to avoid the onset of a resonance condition. The resulting roll amplitude can be rather large depending on the damping level and can lead to ship capsizing in the case of small vessels.
The project thesis examined this phenomenon from theoretical point of view and selected a fishing vessel to carry on a preliminary numerical parameter investigation in terms of incident wave and vessel configuration. The latter concerned the use of cables and their effects on the parametric roll occurrence and features. A cable arrangement is planned to be used on an experimental investigation of the same vessel.

Objective

The aim of the thesis is to provide insights about the sensitivity of the parametric roll occurrence and features on a fishing vessel to the environmental and operational conditions. The occurrence of the parametric roll will be examined numerically using the 6DOF potential-flow solver adopted during the project and also considering an available 1.5DOF method. The more advanced method will be used to continue the parametric study of the phenomenon started during the project. Possibly the investigation will be complemented by including experimental studies on the same fishing vessel.

The work should be carried out in steps as follows:

1. Examine the state of the art in terms of numerical and physical modelling of parametric roll to complete the theoretical investigation performed during the project thesis.
2. Choose a 1.5D model to investigate the parametric roll occurrence for the fishing vessel selected during the project study and compare the results with those from the 6DOF potential-flow model applied. Use the outcomes to discuss the reliability and applicability of the simplified approach.
3. As done during the project, use free decay tests already available for the same fishing vessel but with appendages (bilge keels, skeg, rudder, propeller) to predict the roll damping. Include the damping correction (both as linear and as quadratic correction) into the 6DOF method and check the influence on the occurrence and features of the phenomenon.
4. An experimental campaign is planned on the same fishing vessel with a set of cables to investigate the occurrence of parametric roll. Perform simulations with 1.5DOF and 6DOF methods for the chosen experimental conditions. If possible (a) analyze experimental data in terms of ship motions and (b) compare the parametric-roll occurrence against 1.5DOF, and/or 6DOF, method.

The work may show to be more extensive than anticipated. Some topics may therefore be left out after discussion with the supervisor without any negative influence on the grading.

The candidate should in her report give a personal contribution to the solution of the problem formulated in this text. All assumptions and conclusions must be supported by mathematical models and/or references to physical effects in a logical manner.

The candidate should apply all available sources to find relevant literature and information on the actual problem.

The thesis should be organised in a rational manner to give a clear presentation of the work in terms of exposition of results, assessments, and conclusions. It is important that the text is well written and that tables and figures are used to support the verbal presentation. The thesis should be complete, but still as short as possible. In particular, the text should be brief and to the point, with a clear language. Telegraphic language should be avoided.

The thesis must contain the following elements: the text defining the scope (i.e. this text), preface (outlining project-work steps and acknowledgements), abstract (providing the summary), table of contents, main body of thesis, conclusions with recommendations for further work, list of symbols and acronyms, references and (optional) appendices. All figures, tables and equations shall be numerated.

The supervisor may require that the candidate, in an early stage of the work, present a written plan for the completion of the work. The plan should include budget for the use of computer and laboratory resources that will be charged to the department. Overruns shall be reported to the supervisor.

From the thesis it should be possible to identify the work carried out by the candidate and what has been found in the available literature. It is important to give references to the original source for theories and experimental results.

The thesis shall be submitted in two copies:
- The copies must be signed by the candidate.
- This text, defining the scope, must be included.
- The report must appear in a bound volume or a binder.
- Drawings and/or computer prints that cannot be included in the main volume should be organised in a separate folder.
- The bound volume shall be accompanied by a CD or DVD containing the written thesis in World or PDF format. In case computer programs have been made as part of the thesis work, the source codes shall be included. In case of experimental work, the experimental results shall be included in a suitable electronic format.

Supervisor :Marilena Greco
Submitted :16 January 2013
Deadline :10 June 2013

Marilena Greco
Supervisor

PREFACE

This thesis is a final work on my Master of science study in Maritime Technology at the Department of Marine Technology, Norwegian University of science and Technology, Trondheim. It is part of the Nordic Master in Maritime Engineering program, which includes 1 year of studies in Naval Architecture at Chalmers University, Gothenburg. The thesis is carried out in the Spring Semester of 2013. The subject is Numerical and Experimental Investigation of Parametric Roll.

During the fall 2012 a project thesis was written, which was meant to bring basic understanding and a foundation of the theory and principles for further work covered in this thesis. It is recommendable to read the project thesis first, in order to get full understanding of the problems covered in the master thesis. It is assumed that the reader has some background knowledge to the theory presented in this report.

The 6 DoF solver as well as the 1.5DoF MatLab code were provided by Prof. Marilena Greco and Dr. Claudio Lugni. Small changes were done in the MatLab code in order to obtain the required data for a comparison of a numerical investigation of parametric roll.

The work has been carried out under supervision of Prof. Marilena Greco at the department of Marine Technology, NTNU. Her continuous guidance and quick support is most appreciated.

Trondheim, June 08, 2013

Johannes Geyssel

ABSTRACT

The main purpose of this Master thesis is to provide insights about the sensitivity of parametric roll occurrence. Parametric roll resonance may lead to large roll angles experienced by the ship typically in longitudinal waves. It is related to the periodic change of stability when the ship's wave encounter frequency is approximately twice the rolling natural frequency and the damping of the ship to dissipate the parametric roll energy is not sufficient to avoid the onset of a resonant condition. This study contains a brief description of this physical phenomenon and presents the state of the art in terms of theoretical, numerical and physical modeling.

Using free decay tests, a parameter analysis is carried out, including linear and quadratic damping corrections. The influence of the parametric roll occurrence relative to appendages such as skeg or bilge keels is carried out using the 6DoF potential flow solver. The numerical results are presented as a function in time, showing the amplitudes in heave, roll and pitch.

A 1.5DoF model is chosen to investigate the parametric roll resonance on a fishing vessel. The influence on the occurrence and features of the phenomenon are analyzed using this model. Hence the reliability and applicability of the simplified approach is discussed. Comparing the 1.5DoF model results with experimental results of scaled model testing of the same fishing vessel, a validation of the model is performed, showing that the model is consistent with the experiments.

Contents

List of Figures

List of Tables

1 Introduction

The parametric roll of ships is a well identified problem, and a lot of research has been done to identify the occurrence and characteristics of this phenomenon. Over the last decades many spectacular accidents happened, as for example on the APL China Container vessel in October 1998. The ship encountered an unexpected roll angle of about 40 degrees and lost about one third of the deck containers. Investigations, including numerical simulations and experiments, showed that parametric roll was most likely the cause of damage. This problem can occur on all kind of vessels, including tankers, cruise liners and fishing vessels.

In order to explain this sudden increase in roll amplitude, one has to take a closer look into the roll stability of a vessel relative to the excitation wave. This resonance phenomenon occurs in head and following seas when the wavelength is identical or close to the shiplength. The stability of a ship is reduced if a wave crest is situated amidships. The average waterplane width is significantly lower than in calm water and a total loss of stability may occur. However on a wave trough, the restoring moment is increased and the ship rolls to the other side with an increasing roll angle with time, passing through the vertical upright position. Now the flared parts of the bow and stern are more deeply immersed than in calm water and the wall-sided midship is less deep. An increase of

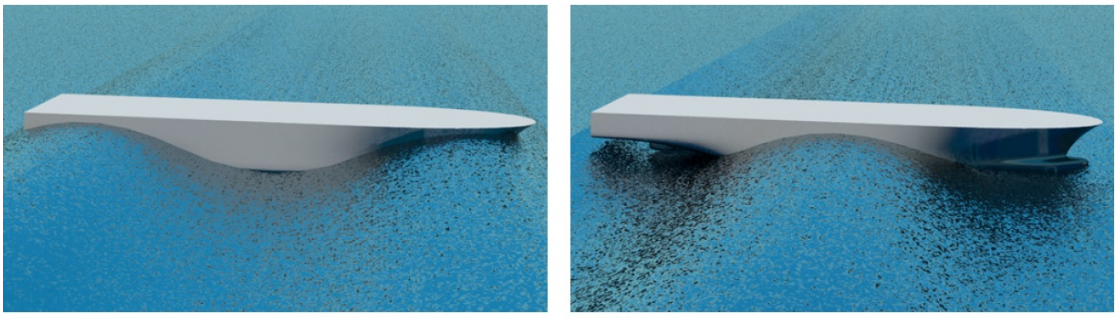

(a) Wave Trough **(b)** Wave Crest

Figure 1.1: Change of waterline in a wave trough (a) and wave crest (b)

the metacentric height (GM) over the calm water is the result. The instantaneous, mean waterplane is now wider than in calm water. This periodic change of the stability (GM), leads to an amplification of the roll amplitude, which in severe cases might lead to capsizing.

This phenomenon occurs at sea states that are usually considered by designers. Clas-

sification societies (e.g. DNV, American Bureau of Shipping) and other regulatories such as IMO have therefore undertaken several activities, in order to introduce the idea that parametrically excited roll motion is more dangerous than the well known resonance rolling motion in beam sea.

There are many different methods to prevent parametric roll. Certain parameters, such as the roll damping and the excitation forces are relevant for parametric roll to start. They have to drop below or exceed threshold values respectively. Consequently, one must consider either increasing the damping or reducing the moment created by the excitation force to prevent the problem. For this reason active and passive roll stabilization devices can be built on. Within this master thesis, passive roll stabilization devices, such as bilge keels and skegs, will be analyzed and compared with the roll motion of the bare hull. The design of such devices is important as they should be over a certain 'effectiveness threshold' to be worth the investment. An example of an active roll stabilization device would be the U–type tank. Two properly sized wing tanks are interconnected via a crossover duct. The resulting fluid flow is used for creating a stabilizing moment opposing the roll motion of the vessel.

Another way to approach this problem is to introduce a decision support system that would inform the shipmaster of foreseen danger. If the ship speed and heading, as well as the sea state is known, it is possible to calculate the upcoming roll motion and prevent dangerous situations. This real-time calculation would however require appropriate hardware to predict the incoming waves and immense computational power. Hence precalculated data could be obtained and presented for vessels in form of polar plots for loading condition and each sea state. As a result the shipmaster would change heading and/or speed or simply alter the route to avoid parametric roll motion.

1.1 Outline

The work starts with the introductory chapter, **chapter 1**, which gives an outline and a brief description of the basic concepts of parametric roll. Motivations are also presented. In order to carry out any further work in any field, it is a necessity to be aware of the latest advancements. Therefore, **chapter 2** provides a review of the state of the art. The methods that are currently in use as well as their limitations and applications are discussed.

After the theory is covered, **chapter 3** introduces the 1.5DoF model that has been used to obtain the numerical results. Its functions, the analytical model as well as the usage are outlined. The input/output files and their structures are detailed.

Chapter 4 introduces the 6DoF potential-flow model. The main features of the model are presented and the mathematical background is described. Previous usage examples of the model are presented.

Chapter 5 gives a full analysis of roll decay tests that were obtained from experimental results from the model tests in the basin of the institute CNR - INSEAN situated in Rome, Italy. A detailed theory of roll damping is given. Furthermore the procedure to obtain damping coefficients is presented as well as the results. Lastly, an analysis of the results for different hull models (bare hull, skeg and bilge keels) using an equivalent damping term or linear and quadratic damping coefficients is carried out.

Chapter 6 investigates the occurrence of parametric roll using a 1.5DoF model, which is implemented into MatLab. The same model characteristics as in chapter 5 (using different appendages) are analyzed. The occurrence of parametric roll is examined by changing the incident wave properties as well as the boundary conditions for fixed-trim or free-trim of the model.

Chapter 7 presents the experimental campaign of the fishing vessel model and gives an overview of the outcome. These results were used to validate the 1.5DoF model.

The work is concluded with **chapter 8**, presenting the general conclusions and discussing possible works.

2 State-of-the-Art

2.1 Introduction

An introduction into the theoretical modeling of parametric roll was already given in the project thesis. However this chapter completes the investigation in terms of theory, and examines the state -of-art in terms of numerical and physical modeling of parametric roll.

2.2 Theoretical background

As already mentioned before, parametric roll is a phenomenon that occurs in longitudinal regular waves (head or following seas). Pitch and heave motions are the result of the direct excitation of the wave and can therefore be described with the linear seakeeping theory. Nevertheless for parametric roll all 6 degrees of freedom will be taken into account. Some approximations however can be done, assuming that the ship is able to keep course, which means that sway and yaw will not change and can be left out. Similarly the surge motion wiiÂ´ll not change, as we expect a constant speed were the ship encounters the same wave frequency. Hence 3 motion remain, i.e. heave, roll and pitch.

The simplest mathematical model of parametric roll can be described with the single degree of freedom motion equation in which the restoring is made nonlinear.

$$\ddot{\phi} + d(\phi, \dot{\phi}) + \omega_0^2[1 + f(t)]\phi = 0 \tag{2.1}$$

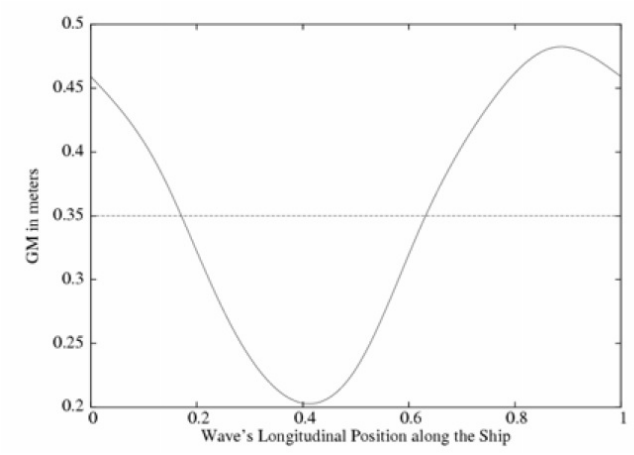

Figure 2.1: Typical GM variation

Where ϕ denotes the roll angle, $d(\phi, \dot{\phi})$ the damping function including the linear and quadratic damping term, ω_0 the natural roll frequency and f(t) denotes the nonlinear restoring coefficient.

Fundamental is to understand how the restoring arm (GZ) is influenced by heave, pitch and wave motions. Knowing these parameters, one can easily calculate the hydrostatic

stability how the GZ curve changes with different Froude numbers. The slope of the restoring arm i.e. the initial metacentric height (the slope $\frac{dGZ}{d\eta_4}$ of the GZ-curve at $\eta_4 = 0$) is the most important. It is largest when the wave trough is mid-ships and smallest when there is a wave crest.

Theoretically if the wave was stationary to the ship and there was a crest midships, this ship could capsize due to static effects only.

Several approximations are possible in order to define and calculate the nonlinear restoring coefficient. The most simple assumption is to set the nonlinear restoring term as a harmonic function of time with a certain amplitude. As the metacentric height GM varies due to the different wave's longitudinal position, one can assume that GM is a periodic function with period T_e. In first order of approximation, the variation can be modeled as a single sinusoidal function with time.

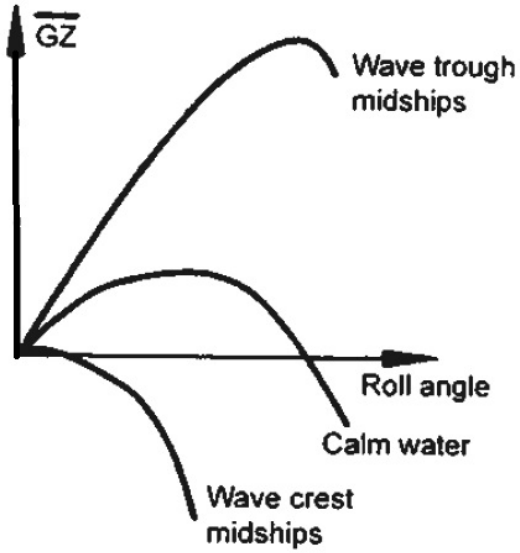

Figure 2.2: Example how the GZ curve is influenced by the wave

$$GM(t) = GM(1 + \delta GM cos(\omega_e t)) \tag{2.2}$$

One typical example of GM variation in waves is shown on figure (2.1). The determination of this curve is not very simple as it depends on many quantities which are nonlinear e.g. heave motion, pitch motion, instantaneous roll angle, instantaneous wave elevation, etc. Inserting this in formula (2.1) one gets

$$\ddot{\phi} + d(\phi, \dot{\phi}) + \omega_0^2[1 + \frac{\delta GM}{GM} cos(\omega_e t)] = 0 \tag{2.3}$$

Relative to the damping function a classical quadratic approximation of the damping moment is considered as

$$d(\phi, \dot{\phi}) = 2p_1\dot{\phi} + p_2\dot{\phi}\left|\dot{\phi}\right| \tag{2.4}$$

where $\dot{\phi}$ denotes the roll angle velocity, p_1 the linear damping coefficient and p_2 the quadratic damping coefficient. The damping component opposes to the roll motion. It

damps and/or dissipates the energy of the motion. In this way a large enough damping moment could prevent the resonance.

Inserting formula (2.4) in (2.3) one gets

$$\ddot{\phi} + 2p_1\dot{\phi} + p_2\dot{\phi}\left|\dot{\phi}\right| + \omega_0^2[1 + \frac{\delta GM}{GM}cos(\omega_e t)] = 0 \tag{2.5}$$

By setting the damping function equal to zero, one gets the Mathieu type instability equation, which is well known in other fields of physics. It allows to define the stability zones of a system. In order to illustrate these zones, one can use the Ince-Strutt diagram on figure (2.3). The unshaded areas represent instability domains with $d(\phi, \dot{\phi}) = 0$. The

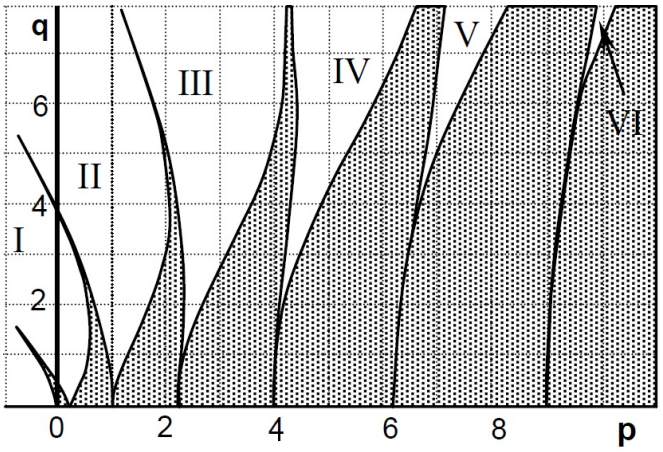

Figure 2.3: Stability diagram for the Mathieu equation

abscissa (q) in this graph represents the ratio of the excitation frequency ω_e(frequency of encounter) and the natural roll frequency ω_0. The ordinate (p), represents the amplitude of GM variation, which is the amplitude of parametric roll excitation. With the parameters p and q, one can easily deduce the critical conditions. The combination of $\sqrt{p} = \frac{\omega_0}{\omega_e} = 0.5, 1.0, 1.5, 2.0$, etc. with low q=$\frac{\delta GM}{GM_m}$ yields to dangerous positions. That means when the excitation frequency is close to twice the natural roll frequency, the stability region is reduced and even small excitation amplitudes may excite the unstable roll motion. In this case damping was neglected. However it will have an positive influence on the stability. The higher the damping, the higher q has to be for instability to occur.

2.3 Numerical modeling

2.3.1 General

In order to predict ships responses by numerical methods, one can roughly divide three different approaches which can be applied to different hydrodynamic problems and type

of vessels. For structures that are very small compared to the encountered wave length, one can use the Morrison equation.

$$F_M = \rho C_m V \dot{u} + \frac{1}{2} C_d A u \left| u \right| \tag{2.6}$$

The first term is the inertia contribution including the inertia coefficient, the volume of the body and the flow acceleration. The second term is the drag contribution which contains the drag coefficient, wetted surface of the body and the flow velocity. The assumption is that the drag force contribution and inertia force contribution are added together linearly. However if the drag contribution is small compared to the inertia forces, then the Froude-Krylov theory can be applied. This can therefore only be done for small structures.

$$F_{FK} = -\int\int_{-S_w} p\vec{n} ds \tag{2.7}$$

Where F_{FK} denotes the Froude-Krylov force, S_w the wetted surface of the floating body, p the pressure in undisturbed waves and $\vec{n}$ the body's normal vector pointing into the water. The formula expresses the product of the wetted surface of the floating body and the dynamic pressure acting from the waves on the body.

Yet if the wavelength has the size of the structure, then a third methodology should be used, which is the diffraction theory. For parametric roll to occur the wavelength has to be the same size or similar to the vessel. In other words, the main focus lies in this theory. It is applicable for slender hull forms, such as long hulled ships but also including fishing vessels. Considering the boundary condition, the Laplace equation is solved using also the so called strip theory. This theory simplifies the three-dimensionality of the structure into a manageable form, in order to achieve quicker solutions in the hydrodynamic calculations.

2.3.2 Strip theory

The strip theory is a method to solve a three-dimensional problem in two dimensions. The three dimensional hydromechanical and exciting wave forces and moments on the ship are computed by integrating the two-dimensional potential solution over the ship length. Interactions between the cross sections are ignored for a zero-speed case. This means that each cross section of the ship is considered to be part of an infinitely long cylinder. Faltinsen and Svensen [3] have discussed this method extensively and they concluded that this method is the most successful and practical tool for calculation of wave induced motions of the ship, at least in an early design stage of the ship.

The ship is considered to be a rigid body, floating in the surface of an ideal fluid, which is incompressible, homogeneous, free of surface tension, irrotational and without viscosity. The specific problem of the motions of the floating body in waves can be linearized. Therefore only the external forces on the underwater part of the ship is considered here and the part of the above water is neglected.

The strip theory is applicable for slender body's and less accurate predictions appear for ships with a low length to breadth ratio. Yet experiments showed that the strip

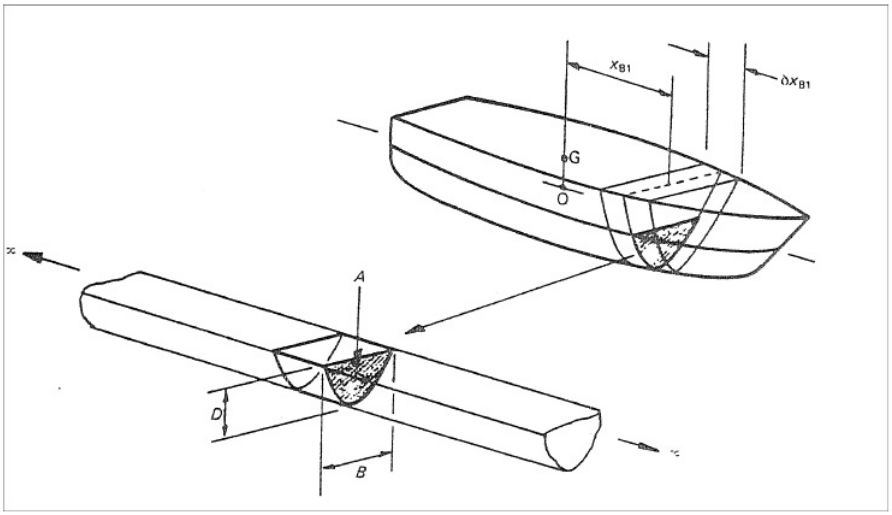

Figure 2.4: The hull is represented by 2D strips

theory appears to be remarkably effective for predicting the motions of ships with length to breadth ratios down to about 3.0, or even sometimes lower. The strip theory is based in the potential flow theory which holds that viscous effects are neglected. This however can deliver some major problems regarding the prediction of roll motion at resonance frequency.

For large ship motions, as they appear in parametric rolling, the strip theory can deliver less accurate results. The so-called "end-terms" become more important. The strip theory is based on linearity, which means that the ship motions are supposed to be small, relative to the cross sectional dimensions of the ship. Only hydrodynamic effects on the hull below the still water are considered. If therefore a part of the ship goes out or into the water, or green water occurs, inaccuracies can be expected.

Anyhow, taking these limitations into account, the strip theory still provides a sufficiently good basis for optimization studies at an early design stage. For more precise results at a later stage, model experiments can be carried out in order to investigate for instance the added resistance or extreme event phenomena.

2.3.3 Time domain numerical modeling of ship motions

The time domain numerical method is an iterative process where the output of the last time step becomes the input for the next time step. Its focus lies in predicting the forces acting on the body and the movements at predefined time steps. For each time step, a new calculation is required to obtain the forces and transcribe them into motions. The underwater part of the hull is also calculated at each time step. To date, the majority of research has assumed that water can be considered as inviscid and incompressible and that the flow around the body remains irrotational. In this case the Laplace equation (2.8) is valid everywhere in the fluid domain and the hydrodynamic forces acting on the

body are determined as the solution to a boundary value problem.

$$\frac{\partial^2 \Phi}{\partial x^2} + \frac{\partial^2 \Phi}{\partial y^2} + \frac{\partial^2 \Phi}{\partial z^2} = 0 \tag{2.8}$$

These are the fundamental assumptions of the potential theory. The standard strip theory can be applied, considering small amplitude motions. The limitation is set due to the underwater geometry that should not change at each time step. For large motions that will not be the case. To overcome this problem one can calculate hydrodynamic coefficients and forces based on the instantaneous conditions. However this increases the computation and modeling time.

The use of time domain analysis is not new, but since the computational power increased, it has become more practical to study actual solutions and investigate the computational advantages of time domain methods. Still, for linear problems at zero forward speed, the time domain computations take more time than the conventional frequency domain approach. More time steps are needed to obtain a few frequencies regarding the frequency domain method. Yet with forward speed, the frequency domain function becomes very difficult to compute and time domain analysis can be significantly faster.

It is also possible to consider a three-dimensional time domain method. Park and Troesch [10] have investigated the stability of time stepping for different two and three-dimensional problems. The conclusions were, that the stability depends upon the geometry of the specific problem, and the integration method. Generally the three-dimensional problems were more stable than two-dimensional problems. The results were closer to the experimental results. However, the simplicity of the two dimensional problems should be considered and time is a very precious factor in engineering. The reliability of strip theory is mostly accurate enough.

2.3.4 Frequency domain numerical modeling of ship motions

For the frequency domain solution of the hydrodynamic problem, one can solve the linear and diffraction problem by various theories. Once again strip theory can be applied. The incoming waves and the forced motions are assumed to be harmonic to simplify the calculations. Hence regular waves are taken in consideration. Also irregular waves can be taken into account. This is done by the superposition principle.

For a ship with forward speed, radiation forces will appear. These forces can be split into one that is in phase with the acceleration and one that is in phase with the velocity. The inviscid damping force is proportional to the damping coefficient and results from the radiation force that is in phase with the velocity of the ship's motion. The other term that is in phase with the acceleration should include the added mass, so that a total equivalent mass is formed. Added mass can be defined as the mass of the fluid that is accelerated by the ship's structure.

The combination of the ship's own weight with the hydrodynamic forces, result in the restoring forces. Usually they can be linearized for simplification (strip theory). The hydrodynamic forces are calculated up to the still water surface. Small changes in the waterplane area of the ship occur. These forces, are the excitation forces, if the ship

is advancing with constant forward speed through a field of incident harmonic waves. The ship is considered to be restrained at its mean position without doing an oscillatory motion. One can divide the forces into two parts, which are the Froude-Krylov forces and the diffraction forces. The latter is related to the perturbation of the incident wave field due to the presence of the vessel itself and the Froude-Krylov force is related to the incident wave field pressure.

Within the frequency domain analysis, it is also possible to compute three-dimensional solutions. In this case strip theory is not applicable. This increases the computational power drastically, since the problem becomes more complex. The main difference from strip theory is, that a 3D panel method can be applied to all structures even if the body is not considered slender.

Transfer functions

In order to find the response of a ship or platform in the frequency domain, one can calculate the transfer function. Here linear theory is assumed which implies that the motions are proportional to the wave amplitude. The transfer function gives the ratio between the amplitude of a given motion of the ship and the wave amplitude as a function of frequency. Moreover the transfer function can also serve as an indicator for testing a computer program, since one can easily compare the transfer functions for a given ship to a transfer function of a new developed program or experimental tests.

Firstly one has to find the steady state amplitude for the motion of interest. In this case the roll motion, which we find from the particular solution. Assume that the body is forced to oscillate in roll in calm water with the amplitude η_4 and the angular frequency ω.

$$\eta_4 = \widehat{\eta}_4 e^{i\omega t} \tag{2.9}$$

The roll angular velocity is then

$$\dot{\eta_4} = -i\omega\widehat{\eta}_4 e^{i\omega t} \tag{2.10}$$

and the roll angular acceleration

$$\ddot{\eta_4} = -\omega^2\widehat{\eta}_4 e^{i\omega t} \tag{2.11}$$

Regarding all the motions without forward speed, one can express the equation of motion in matrix form as

$$\eta = \begin{bmatrix} \eta_2 \\ \eta_3 \\ \eta_4 \\ \eta_5 \\ \eta_6 \end{bmatrix}$$

The equation of motions requires also the mass matrix, which can be set up as following (Faltinsen 2005)

$$M_{jk} = \begin{bmatrix} M & 0 & -Mz_G & 0 & 0 \\ 0 & M & 0 & 0 & 0 \\ -Mz_G & 0 & I_4 & 0 & -I_{46} \\ 0 & 0 & 0 & I_5 & 0 \\ 0 & 0 & -I_{46} & 0 & I_6 \end{bmatrix}$$

where I_j is the moment of inertia in the jthmode and I_{jk} is the product of inertia with respect to the coordinate system. The added mass matrix is given as

$$A_{jk} = \begin{bmatrix} A_2 & 0 & A_{24} & 0 & A_{26} \\ 0 & A_3 & 0 & A_{35} & 0 \\ A_{42} & 0 & A_4 & 0 & A_{46} \\ 0 & A_{53} & 0 & A_5 & 0 \\ A_{62} & 0 & A_{64} & 0 & A_6 \end{bmatrix}$$

and damping matrix respectively according to (Salvesen er al., 1970).

$$B_{jk} = \begin{bmatrix} B_2 & 0 & B_{24} & 0 & B_{26} \\ 0 & B_3 & 0 & B_{35} & 0 \\ B_{42} & 0 & B_4 & 0 & B_{46} \\ 0 & B_{53} & 0 & B_5 & 0 \\ B_{62} & 0 & B_{64} & 0 & B_6 \end{bmatrix}$$

Further the matrix containing the linear restoring coefficients is

$$C_{jk} = \begin{bmatrix} 0 & 0 & 0 & 0 & 0 \\ 0 & C_3 & 0 & C_{35} & 0 \\ 0 & 0 & C_4 & 0 & 0 \\ 0 & C_{53} & 0 & C_5 & 0 \\ 0 & 0 & 0 & 0 & 0 \end{bmatrix}$$

The last matrix is the excitation matrix which is given as

$$F = \begin{bmatrix} F_2 \\ F_3 \\ F_4 \\ F_5 \\ F_6 \end{bmatrix}$$

Now the equation of motion can be written as

$$(M + A)\ddot{\eta} + B\dot{\eta} + C\eta = Fe^{i\omega_e t} \tag{2.12}$$

where ω_e denotes the encounter frequency and the forces in the matrix (2.12) are written in complex form $x + iy$. The phases of each force are taken into account by the real and

imaginary parts.

As in equation 2.9 for the roll motion, one can write in general form, assuming once again that all modes of motion are oscillating harmonically. The response matrix can be written as

$$\eta = \widehat{\eta} e^{i\omega t} \tag{2.13}$$

$$\dot{\eta} = -i\omega \widehat{\eta} e^{i\omega t} \tag{2.14}$$

$$\ddot{\eta} = -\omega^2 \widehat{\eta} e^{i\omega t} \tag{2.15}$$

where $\widehat{\eta}$ is the complex motion amplitude. One can now insert the equations 2.13, 2.14, 2.15 in 2.12 which then becomes

$$-\omega_e^2 (M + A)\widehat{\eta} e^{i\omega t} + i\omega B \widehat{\eta} e^{i\omega t} + C\widehat{\eta} e^{i\omega t} = F e^{i\omega t} \tag{2.16}$$

This equation (2.16) is a function of frequency and independent from time. One can now write the complex response matrix as

$$\widehat{\eta}(\omega) = H(\omega) F(\omega) \tag{2.17}$$

where $H(\omega)$ is called the mechanical transfer function which is defined as

$$H(\omega) = [-\omega_e^2 (M + A) + i\omega_e B + C]^{-1} \tag{2.18}$$

For each mode, the final response amplitude is given by the absolute value of the complex response amplitude with

$$\eta_j = \sqrt{\eta_{Rj}^2 + \eta_{Ij}^2} \tag{2.19}$$

where R stands for the real part,I the imaginary and j goes from 2...6. The phase angle between the response and load can be found by the ratio of the real and imaginary part

$$\epsilon_j = arctan \frac{\eta_{Ij}}{\eta_{Rj}} \tag{2.20}$$

An example of a transfer function in roll for beam sea with and without forward speed is given on figure 2.5. One can see that for long waves the value of the transfer function goes towards 1 and for short waves to 0. This shows that the calculations are realistic and follow a physical behavior. For $U = 0$ knots, one can see that when the wave frequency ω reaches the natural roll frequency ω_0 a large roll motion occurs.

2.4 Experimental modeling

Experimental model testing of ships has a long tradition. Improved resistance performance was the early start of the development of ship model testing. By doing so, simple methods could give recommendation about which shape of ship gives the highest speed.

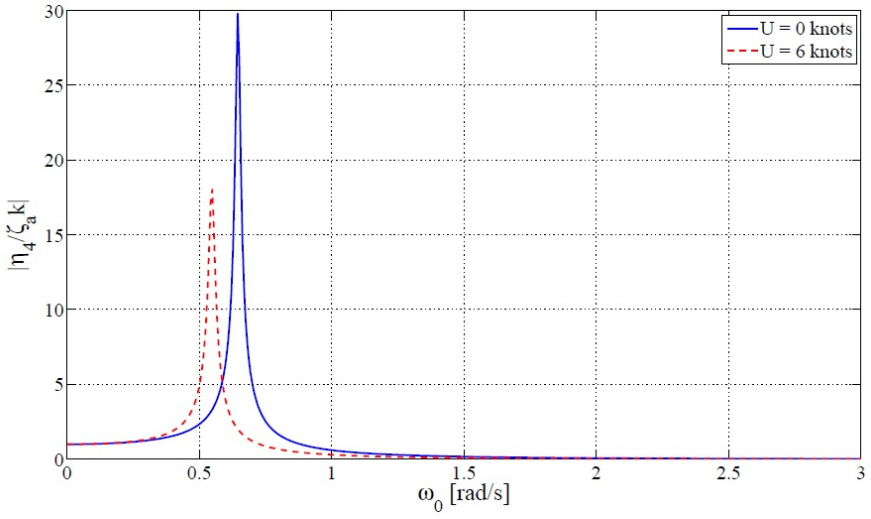

Figure 2.5: Example of roll transfer function (Martinussen, 2011)

This idea can be transferred into many other aspects, including the stability of ships. As physical models are intended to represent the full-scale system as good as possible, one has to fulfill the general modeling laws. First laws were introduced by William Froude (1810-1897) regarding the model resistance to the actual ship resistance.

To achieve similarity in forces between the model and full scale situation the following conditions has to be fulfilled:

Geometrical similarity defines, that geometrical similar structures should have the same shape in model scale as well as full scale. That means that a constant length characteristic must remain constant, i. e.

$$\lambda = L_f / L_m \tag{2.21}$$

Where λ denotes the scale factor and L_m,L_f any dimensions of the model/full scale structure. The requirement to equal length ratio for all dimensions does not only apply on the ship, but should also be fulfilled to the surrounding environment. Uncertainties and difficulties to fulfill these requirements might appear in some cases, for example regarding the actual surface roughness of a ship which cannot be accurately modeled. Another example is the almost unrestricted extent of the surrounding water. Yet the water depth is easier to model as the dimensions are smaller.

Kinematic similarity includes the equality of the velocity ratios in model and full scale. This implies that the flow will undergo the geometrical similar motions in both cases. For example the ratio between the forward speed of a ship and the rotational speed of the propeller has to be the same:

$$\frac{V_f}{n_f(2\pi R_f)} = \frac{V_m}{n_m(2\pi R_m)} \tag{2.22}$$

or

$$\frac{V_f}{n_f D_f} = \frac{V_m}{n_m D_m} \rightarrow J_f = J_m \tag{2.23}$$

where V is the ship speed, n is the rate of revolution of the propeller, R the radius of the propeller, D the propeller diameter and J the advance coefficient.

Dynamic similarity is achieved if the same force contributions in the problem have the same ratio as in model and full scale. The main forces are referred to:

- Inertia forces
- Viscous forces
- Gravitational forces
- Pressure forces
- Elastic forces in the fluid
- Surface forces

Considering elastic cables, the elastic relative deformations scaling has to be taken into account.

In order to compare the two systems/ships in a simple manner, one can use the dimensionless numbers. The most important and widely used are:

Froude number which is applied on the ratio between inertia and gravity forces. Regarding the model and full scale comparison one can write

$$F_n = \frac{U_m}{\sqrt{gL_m}} = \frac{U_f}{\sqrt{gL_f}} \tag{2.24}$$

where F_n denotes the Froude number. If geometrical and kinematic similarity are fulfilled, then in addition with equality in Froude number one can ensure similarity between inertia and gravity forces. Regarding the wave resistance coefficient, one can say that both are equal, since surface waves are gravity waves.

Reynolds number will give an equal ratio between inertia and viscous forces:

$$Re = \frac{U_m L_m}{\nu_m} = \frac{U_f L_f}{\nu_f} \tag{2.25}$$

where Re is the Reynolds number and ν the kinematic viscosity of the fluid. Equality in Reynolds number will therefore ensure that the viscous forces are correctly scaled in model and full scale.

Webers number includes the ratio between inertia and surface tension forces.

$$We = \frac{U_m}{\sqrt{\frac{\sigma_m}{\rho_m L_m}}} = \frac{U_f}{\sqrt{\frac{\sigma_f}{\rho_f L_f}}} \tag{2.26}$$

The quantity is useful in analyzing thin film flows and the formation of droplets and bubbles i.e cavitation.

More dimensionless numbers exist that are used in scaling for experimental methods. These are for example the Mach's number (force ratio of inertia to elasticity), Keulegan-Carpenter number (force ratio of drag to inertia), Strouhall number (non-dimensional vortex shedding frequency), etc.

In practice it is not possible to satisfy all different scaling laws simultaneously. For ships the most practical situations are influenced by the surface wave effects. This includes incoming waves generated by forward speed or motions of the ship. The surface wave formation is governed by the gravitational forces. Therefore it is necessary to achieve equality in Froude number in model and full scale. However if viscous forces are more important for the actual situation, then one has the requirement to achieve equality in Reynolds number. Scaling both dimensionless numbers is not possible. Hence in conventional experimental model testing of ships and offshore structures Froude scaling is used, although the viscous forces will not be correctly scaled. Post-calculations and other correction methods are used to adjust the effect of differences in Reynolds number.

2.4.1 Model tests vs. Numerical calculations

In table 2.1 one can see the most important qualities of experimental model testing and numerical models. The weighting in the table represents a general evaluation of the capabilities of two different tools. The assessment depends on the actual case, the complexity of the problem and how appropriate the numerical code as well as the test facility is for the actual case.

Qualities	**Physical Models**	**Numerical Models**
Representation	Very good	Limited by available theories and computer power
Accuracy	Good	Good within validity limits
Reliability	Very good	Risk of human errors
Credibility	Very good	Prima facie not good
Flexibility	Not good	Good
Execution	Long	Low with standard programs
Cost	High	High development cost

Table 2.1: Physical versus Numerical Models (from Aage (1992))

One of the main advantages is that model testing is capable of analyzing very complicated situations. Furthermore one can be sure that all important physical phenomena are properly covered. This can be very helpful, especially for new design solutions or innovative concepts. However the lack of flexibility can be a problem. This includes changing design conditions, costs and scale effects.

Nowadays, numerical calculations become more accurate and easier to use, which reduces the importance of experimental testing for routine verification of the performance of ships. Despite calculations are slowly taking over the routine work, still new and technologically demanding structures need experiments in order to analyze or confirm numerical methods.

3 1.5DoF model

3.1 Introduction

As prior mentioned in chapter 2 (State-of-the-art), one can say that a ship that is sailing in upright position in longitudinal regular sea is subjected to the actions of symmetrical motions and waves. When analyzing the problem of parametric roll occurrence, all 6 DoF should be considered as coupled, since large motion amplitudes appear. Regarding a simplified model, one can neglect the sway and yaw motion, as it is assumed that the model keeps course (on average). Also the surge motion can be neglected, assuming the ship is able to maintain a constant speed. Thus only 3 motions remain: heave, roll and pitch.

The remaining three motions are coupled with each other. One can determine the influence of roll to heave and pitch as an explicit forcing with a frequency twice the roll frequency. On the contrary the influence of heave and pitch on roll can be seen as a parametric excitation. Regarding a constant displacement of the vessel, one can write the roll motion equation as follows:

$$\ddot{\phi} + d(\phi, \dot{\phi}) + \omega_0^2 \frac{\overline{GZ}(\phi, \vartheta, \eta, x_c)}{\overline{GM}} = 0 \tag{3.1}$$

where ϕ is the roll angle, ϑ the pitch angle, η the heave displacement and x_c the wave crest position along the ship. Assuming that the heave and pitch motion are functions of the roll angle and the position of the wave crest, one can simplify the restoring term as

$$\overline{GZ}(\phi, \vartheta, \eta, x_c) = \overline{GZ}(\phi, x_c) = \overline{GZ}(\phi, t) \tag{3.2}$$

Knowing the ship speed, the wave celerity and the encounter angle of the wave, one can obtain the explicit dependence on time. In order to fulfill the assumption in equation 3.2, that is, to explain the dependence of pitch and heave to roll, one should in principle introduce additional coupled equations. This would need complex analytical approximate techniques with high order non-linearities. The more simple option is to introduce a quasi static assumption, meaning that heave and pitch are assumed to be statically balanced in wave. The restoring moment is calculated according to a standard hydrostatic software where non-hydrostatic effects are neglected.

Two different cases can be calculated using this method: The 'free-trim' or 'fixed trim' methodology. When a 'free-trim' is used, then both sinkage and trim are free to move. However using the 'fixed-trim', the trim is kept constant, while the sinkage is still free to vary. These are two approaches to determine the hydrostatic hull pressure under the wave

profile. Presently the IMO requires free trim calculations. Regarding the assumptions prior mentioned, it is to be said, that in some range the results are more accurate. This will be the case for following waves (low encounter frequencies) and a wavelength that is identical or larger that the ship.

3.2 Analytical model

The analytical model used in this analysis is given when inserting equation 3.2 into 3.1. The model includes a varying restoring lever GZ dependent on wave crest position and heeling angle. The so called 1.5 DoF roll motion equation can be written as

$$\ddot{\phi} + d(\phi, \dot{\phi}) + \omega_0^2 \frac{\overline{GZ}(\phi, x_c)}{\overline{GM}} = 0 \tag{3.3}$$

where

- $\ddot{\phi}$ roll angle acceleration
- $d(\phi, \dot{\phi})$ damping function
- ω_0 the natural roll frequency
- $\overline{GZ}(\phi, x_c)$ the restoring lever in waves
- $\overline{GM}$ the still water metacentric height
- x_c the wave crest position

The 1.5 degrees of freedom are decomposed of 1 DoF for the roll motion and an additional 0.5 DoF as a reminder for the simplified static accounting for sinkage and trim (heave and pitch). The restoring lever GZ contains information about the heeling angle as well as the position of the wave crest. By using the quasi static assumption, one can evaluate the restoring lever for each position of the wave crest along the hull. The wave is regarded to be frozen, while the restoring moment is evaluated for different heeling angles. This can be done using the fixed or free trim approach, whereas the displacement is kept constant.

The term $\overline{GZ}(\phi, x_c)$ can be written as a Fourier series. This can be done by first approximating the term, for each wave crest position, by means of the least square polynomial fitting with degree N_p:

$$\overline{GZ}(\phi, x_c) \approx \sum_{j=0}^{N_p} A_j(x_c)\phi^j \tag{3.4}$$

Assuming a wave length λ_w and a sea that is exactly longitudinal (head or following seas), one can write a periodicity condition that holds

$$A_j(x_c) = A_j(x_c + n\lambda_w) \qquad \text{with} \qquad n = 0, \pm 1, \pm 2, ... \tag{3.5}$$

This condition (equation 3.4) allows to express each coefficient $A_j(x_c)$ as a Fourier series. It contains a main period λ_w and a variable x_c:

$$A_j(x_c) = A_{j0} + \sum_{n=1}^{N_h} A_{jn}^c cos(k_n x_c) + A_{jn}^s sin(k_n x_c) \tag{3.6}$$

This Fourier series has a maximum number of harmonic components N_h, which can be estimated from $A_j(x_c)$. It depends on the position number at which $\overline{GZ}(\phi, x_c)$ is evaluated. Furthermore k_n denotes the wave number, being

$$k_n = nk_w = n\frac{2\pi}{\lambda_w} \tag{3.7}$$

By introducing the Fourier series coefficients: initial, sinus and cosinus

$$A_{j0} = \frac{1}{\lambda_w}\int_0^{\lambda_w} A_j(x_c)dx_c \tag{3.8}$$

$$A_{jn}^c = \frac{2}{\lambda_w}\int_0^{\lambda_w} A_j(x_c)cos(kx_c)dx_c \tag{3.9}$$

$$A_{jn}^s = \frac{2}{\lambda_w}\int_0^{\lambda_w} A_j(x_c)sin(kx_c)dx_c \tag{3.10}$$

one gets a combining expression for the approximation of $\overline{GZ}(\phi, x_c)$, being

$$\overline{GZ}(\phi, x_c) \approx \sum_{j=0}^{N_p} \left\{A_{j0} + \sum_{n=1}^{N_h} A_{jn}^c cos(kx_c) + A_{jn}^s sin(kx_c)\right\}\phi^j \tag{3.11}$$

It is to be mentioned, that the still water righting arm does not coincide with the mean value of $\overline{GZ}$ in waves, especially for large wave amplitudes. Also for the metacentric height $\overline{GM}$ a term can be determined as a function of the wave crest position x_c. If assumed $\phi = 0$ then one can write

$$\overline{GM}(x_c) = \frac{\partial \overline{GZ}(\phi, x_c)}{\partial \phi}\Big|_{phi=0} \approx A_{10} + \sum_{n=1}^{N_h} A_{1n}^c cos(kx_c) + A_{1n}^s sin(kx_c) \tag{3.12}$$

In order to reach the fully analytical differential equation for the nonlinear parametric roll from BULIAN [5], one can insert equation 3.12 into 3.3, and get

$$\ddot{\phi} + d(\phi, \dot{\phi}) + \frac{\omega_0^2}{\overline{GM}} \sum_{j=0}^{N_p} \left\{A_{j0} + \sum_{n=1}^{N_h} A_{jn}^c cos(kx_c) + A_{jn}^s sin(kx_c)\right\}\phi^j \tag{3.13}$$

In the next step the analytical model will be recasted in time domain. Some major simplifications can be made, since the master thesis only analyzes certain cases. Here the ship is seen as fixed and no forward motion is considered. The reference system stays

therefore the same and can be seen as fixed. Furthermore only longitudinal sea is taken into account (i.e. head or following sea). The wave crest position is when t=0 equal to the reference system position:

$$x_{c0} = \frac{\xi_{c0}}{cos(\chi)} = \xi_{c0} \qquad \text{for} \qquad \chi = 0deg \quad \text{and} \quad 180deg \tag{3.14}$$

Generally one can write the wave crest position as a function of time, being

$$x_c = x_{c0} + (c_w - V_s)t \tag{3.15}$$

where V_s is the ship speed and equal to zero for no forward speed. In this case also the wave frequency is equal to the encounter frequency. Therefore the wave celerity c_w is obtained by $c_w = \omega_w / k_w$.

BULIAN [5] transforms the coefficients into

$$Q_j(t) = A_j(t)$$
$$Q_{j0} = A_{j0}$$
$$Q^c_{jn} = A^c_{jn} cos(n\psi_{c0}) + A^s_{jn} sin(n\psi_{c0})$$
$$Q^s_{jn} = -A^c_{jn} sin(n\psi_{c0}) + A^s_{jn} cos(n\psi_{c0}) \qquad \text{with} \qquad \psi_{c0} = 2\pi \frac{x_{c0}}{\lambda_w}$$

including information for the wave crest position. The information for the wave direction, ship speed and encounter frequency will be implemented afterwards. This however is not of main interest and on that account the thesis will not go into further details.

3.3 Numerical implementation of the analytical model

For the implementation of the analytical model, the numerical computing environment MatLab is used. Many subroutines are built in into one main program, which calculates the hydrostatics features of a certain case. The first step is to load the ship's dimensions, which in the case of this thesis is a fishing vessel with a geometry explained in chapter 7.

After implementing the geometry of the hull, the restoring lever $\overline{GZ}(\phi, x_c)$ is evaluated. This is done for a certain amount of positions of the wave along the hull. It starts from the aft perpendicular ($x_c = 0$) and moves upfront to the last position, which corresponds to the same wave crest at $x_c = \lambda_w$. For each position a set of heeling angles are analyzed, which are from 0deg to 55deg with a step of 2.5 deg. By doing so, a surface matrix is created which contains the curve of $\overline{GZ}(\phi, x_{c,i})$, where i stands for the crest position.

In the next step, a polynomial approximation of each column of the matrix is done, that is for each wave crest position. In order to reach a transient restoring lever with a step of 1deg, the $\overline{GZ}$ curve will be resampled by means of cubic spline interpolation. This interpolation is preferred, so that the interpolation error is small, even for low degree polynomials. It avoids the problem of the Runges phenomenon [11]. The metacentric height ($\overline{GM}$) is a linear coefficient that is not obtained from the least square method

(contrary to $\overline{GZ}$). It means that the coefficient $A_1(x_{c,i})$ is estimated from the numerical derivative of the restoring lever curve, close to the upright position at $\phi = 0$. On figure 3.1, one can see that then a new matrix is created, in order to substitute the previous one. By doing so the i-th column contains the coefficients $A_j(x_{c,i})$. As a next step a

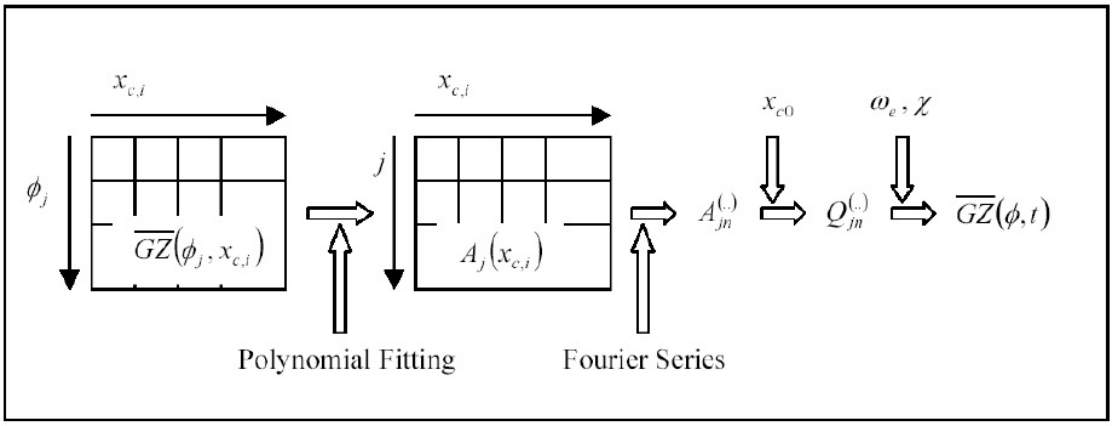

Figure 3.1: Scheme of the steps used for the implementation of the mixed polynomial-Fourier approximation of restoring lever in waves - from BULIAN [2005]

Fourier transformation is made for each coefficient $A_j(x_{c,i})$. A discrete Fourier transform algorithm is used to analyze the polynomial coefficients as a function of the wave crest position. Including the information of the initial wave crest position in time domain, one can lastly calculate the $Q_{jn}^{\cdot\cdot}$ coefficients. By changing the input parameters of the encounter wave frequency and wave heading, one can obtain the requested restoring lever in waves in time domain $\overline{GZ}(\phi, t)$.

3.4 Fixed trim vs. Free trim

Another feature of the 1.5 DoF model is the possibility to change the boundary conditions for trim. As already mentioned before, one can use a 'free-trim' approach where both, sinkage and trim of the vessel are free, or 'fixed-trim', where only the sinkage is free to vary. These two approaches represent the two old possible ways of performing hydrostatic calculations for intact ships and will be later on compared with each other regarding the occurrence of parametric roll.

Comparisons with experimental results in regular sea, show that the 'free-trim' approach in all cases underestimates the amplitude of motion and the range of speeds where instability of the upright position is observed. The 'fixed-trim' on the other side is able to give good predictions in the amplitudes of roll in terms of peak, while the description of the shape might not be satisfactory.

4 6DoF potential-flow model

In order to compare the different damping characteristics of the experimental decay tests, a numerical solver is used that was already introduced in the project thesis, written in the autumn semester 2012. This solver, provided by Prof. Marilena Greco, is a 6DoF numerical algorithm based on potential flow assumptions.

4.1 Main features of the model

The numerical solver used to analyze the parametric roll occurrence as a function of the damping is a 3-D seakeeping analysis model. This model was developed to handle occurrence and effects of water-on-deck and bottom slamming. It is divided into three parts that are coupled with each other

1. the rigid ship motions
2. the water flowing along the deck
3. bottom slamming events

While part 2 and 3 are not of main interest for parametric rolling, the focus lies merely on part 1.

As mentioned before, the numerical solver takes all 6 degrees of freedom into account and it is based on potential flow assumptions. This implies that the velocity field can be considered as irrotational and the fluid incompressible. Also forward motion of the ship (with limited speed) as well as the ship interaction with regular and irregular sea states can be studied. However, regarding the analysis of parametric rolling, no forward motion of the ship will be considered, only longitudinal waves (wave frequency = encounter frequency) and regular sea states.

The rigid body equation of motion are given by Newtons second law and in order to keep the ship generalized mass matrix constant in time, they are written along the body coordinate system. The ship is assumed free to move in 6 degrees of freedom $\xi = (\xi_1, \xi_2, \xi_3, \xi_4, \xi_5, \xi_6)$ (see figure 4.1), while the elastic deformations are neglected. The six component vector equation is given as

$$M\ddot{\xi} + \Omega \times M\dot{\xi} = F \tag{4.1}$$

where Ω denotes the angular velocity vector including $\dot{\xi}_4, \dot{\xi}_5, \dot{\xi}_6,$. These velocities are time derivatives of the motions, along the instantaneous body axes. The cross product of the angular velocity and $M\dot{\xi}$ will give a six component vector. The forces and

moments, represented by the term F in equation 4.1, are the external loads causing the body motions. Disregarding the water on deck and slamming, F is decomposed as $F_g+F_{0nlin}+F_{hnlin}+F_{rsc}$. These loads are connected to the ship weight, the Froude-Krylov force, restoring and radiation-scattering contributions. The solution of the seakeeping

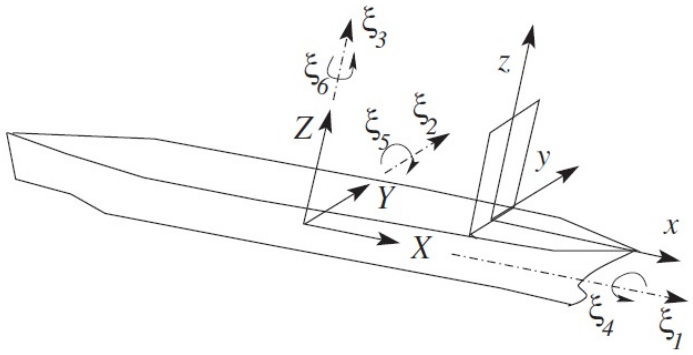

Figure 4.1: Reference frame in the center of gravity and ship motions, ξ_1, surge; ξ_2, sway; ξ_3, heave; ξ_4, roll; ξ_5, pitch; ξ_6, yaw

problem is based on the wake-scatterer hypothesis. This implies that the waves radiated from the ship are small relative to the incoming wave amplitude. Moreover the incident disturbances are considered small with respect to the ship rigid motions. By solving the linear radiation problem about the mean free surface and body surface, instead of the instantaneous incident wave, it is possible to obtain the solution through the frequency domain approach. Due to the quadratic velocity contributions, which are included in the Froude-Krylov and hydrostatic pressure, the forces F_{0nlin} and F_{hnlin} have non-linear terms. This results from the incident waves and ship body motions, which are evaluated on the instantaneous wetted body configuration. The incident waves acting on the body, concerning regular sea waves, are described by second-order Stokes waves. Lastly, the radiated and scattering force F_{rsc} is referred to the disturbance to the wave field due to the presence and motion of the ship.

Regarding the solution in equation 4.1, M is given in the ship mass properties and the generalized forces are evaluated at any time instant i.e.in this case: $F_g, F_{0nlin}, F_{hnlin}$. By projecting the gravitational loads in the instantaneous body reference frame, one gets F_g. If all generalized forces are known at any time instant, then equation 4.1 can be integrated so the ship motions (ξ) and velocities ($\dot{\xi}$) are available. This is done by the fourth order Runge-Kutta [1]. The estimated ship velocities can then be expressed in the inertial reference frame and then integrated in order to get the motions.

This fully 3-D seakeeping solver has already been used to analyze parametric roll on a FPSO in combination with water on deck. The solver provides results globally consistent with the experiments, with a good agreement in terms of motion amplitudes, especially

for the roll. The major discrepancies in terms of phenomena occurrence are documented for cases more sensitive to the involved non-linearities and so to the numerical approximations [2].

5 Decay test

5.1 Introduction

When a ship is in calm water, any disturbance in transversal will lead to roll motions. This can come from any physical natural excitation in full scale, such as wind and waves. In order to get the decay tests in model experiments, usually a single excitation is given and the decay is measured over time. When the roll equilibrium is disturbed, the hydrostatic restoring moment acts to oppose the instantaneous roll angle and tends to return the ship back to the upright position. Due to the inertia of the ship, it does not stop at the instant when the equilibrium angle is reached but continues to roll with a slower velocity until its maximum roll angle is reached. Then the restoring moment causes the ship to begin to right itself. Once upright, inertia causes the ship to continue to roll. This motion cycle is repeated all over again and in theory is only limited by the damping. The period of the roll oscillation in calm water is known as the natural roll period and natural frequency, respectively.

5.2 Roll damping

The roll motion causes waves that radiate out from the body, and the moment, $B_4\dot{\eta}_4$, needed to keep this radiation is in phase with the angular velocity. These radiated waves transport energy away from the body and thus introduces hydrodynamic or radiation damping. The roll motion is however not dominated by the radiation damping, but depends more on turbulent skin friction, turbulence caused by bilge keels and appendages. This means that the total damping cannot be calculated by potential theory only, but also other damping contributions must be taken into account. Normally one uses experiments, which however come with obvious problems of scaling. Viscous and turbulence flow computations have been created in order to correct these problems. One can say that the roll-damping moment is caused by:

- radiated waves
- turbulent skin friction between hull and water
- appendage or bilge keel vortex shedding
- moorings for moored ship or platforms

Besides the first point, the contributions of the roll damping moment are functions of the velocity squared, which means they depend on the amplitude of the roll. Fishing vessels

are floating bodies in the water surface, yet the radiation roll damping is a function of the frequency of oscillation due to the generation of waves. In the limit $\omega \to \infty$ no waves can be formed and the radiation damping is equal to zero. Hence, no surface gravity waves are produced. Also for $\omega \to 0$ the radiation damping will be zero. Consequently, a maximum is somewhere in between where the body has a maximal ability to radiate energy or absorb wave energy.

From the stability point of view it is preferable to have a high damping component in order to reduce the roll motions. In general, roll damping tends to be small for monohulls. Viscous and wave-generation roll damping is present on the bare hull of every vessel. It can be increased/decreased by changing the hull form. The frictional force is resisting the roll motion in the opposite direction together with a wave-generation component. The relatively small roll damping caused by the bare hull is counteracted in conventional fishing vessels, for instance, using bilge keels, skegs and antirolling tanks. Fins and rudders cause a roll damping that increases with speed. In order to describe how the model behaves at certain conditions, one has to find the damping characteristics of the ship. This can be done by finding the damping coefficients and inserting them in the equation of motion. To find the damping coefficients we use the experimental data obtained from the model testing that was performed in a ship model basin of the institute CNR - INSEAN situated in Rome, Italy. For this reason, the model was excited and the decay of the motions was recorded over time.

Decay tests will give important information about natural frequencies, added mass and as mentioned before, the damping of a dynamic system. We start by considering a system with one degree of freedom and non-linear damping. The differential equation describing the motion is

$$M\ddot{x} + B_1\dot{x} + B_2\dot{x}\,|\dot{x}| + Cx = 0 \tag{5.1}$$

Here M is the mass, including added mass, B_1 is the linear damping, B_2 is the quadratic damping term and C the restoring stiffness. The natural frequency of the system can easily be found with

$$\omega_0 = \sqrt{\frac{C}{M}} \tag{5.2}$$

To determine the linear and non-linear damping the equation of motion (5.1) is divided by the mass and one gets the following equation

$$\ddot{x} + p_1\dot{x} + p_2\dot{x}\,|\dot{x}| + p_3x = 0 \tag{5.3}$$

The linear and quadratic damping term can now be determined from the relation

$$\frac{2}{T_m}log(\frac{X_{n-1}}{X_{n+1}}) = p_1 + \frac{16X_n}{3T_m}p_2 \tag{5.4}$$

where X_n is the amplitude of the n-th oscillation. By plotting the left hand side against the equivalent velocity $\frac{16X_n}{3T_m}$, the equivalent damping coefficient can be found. The coefficient p_1 is found from the figure from the intersection to the axis (abscissa) and p_2 is found from the slope of the straight line that was fitted through the values by the least square method.

5.3 Obtaining the damping coefficients

As explained before, the model is excited and the roll decay is measured over time. Although calculations were already done in the project thesis, the aim for this master thesis is to get more accurate results. The procedure starts by measuring the model roll decay without any appendages, i.e. bare hull:

1. Find the natural roll frequency from the roll decay data using formula (5.2)
2. Calculate $\frac{16X_n}{3T_m}$ for each period T_m
3. Calculate $\frac{2}{T_m}log(\frac{X_{n-1}}{X_{n+1}})$ for each period T_m
4. Plot 3) over 2) and fit a curve with the linear least-square method
5. Extract p_1 and p_2 from the plot

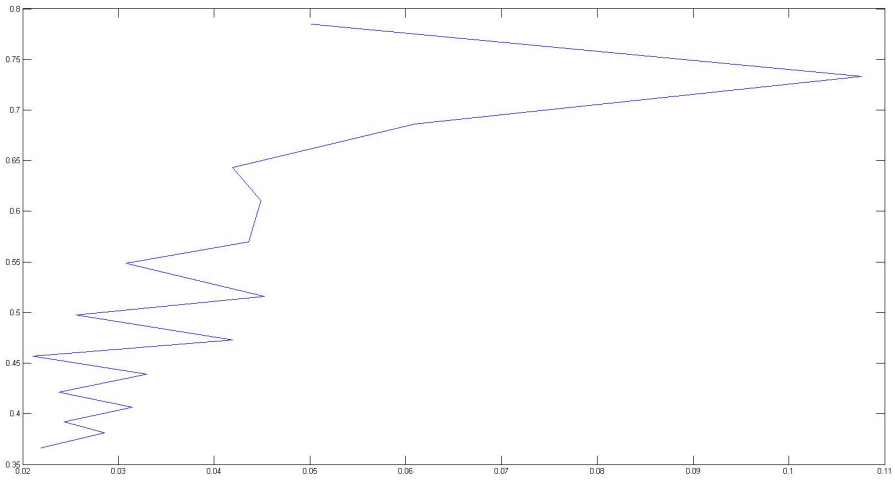

Figure 5.1: Step 4 before fitting a curve

This has been done 7 times, due to 7 different and independent measurements. The aim is to reduce the uncertainties and get more accurate results. On figure 5.2 one can see

that some measurements do not follow a certain trend. These values should be kept outside the calculations. One should avoid using the first oscillation due to transient effects and the smallest amplitudes at the tail of the decay due to inaccuracy. After evaluating the data one can fit a curve simply using the MatLab curve fitting tool ($tftool$) and read p_1 and p_2 from the figure.

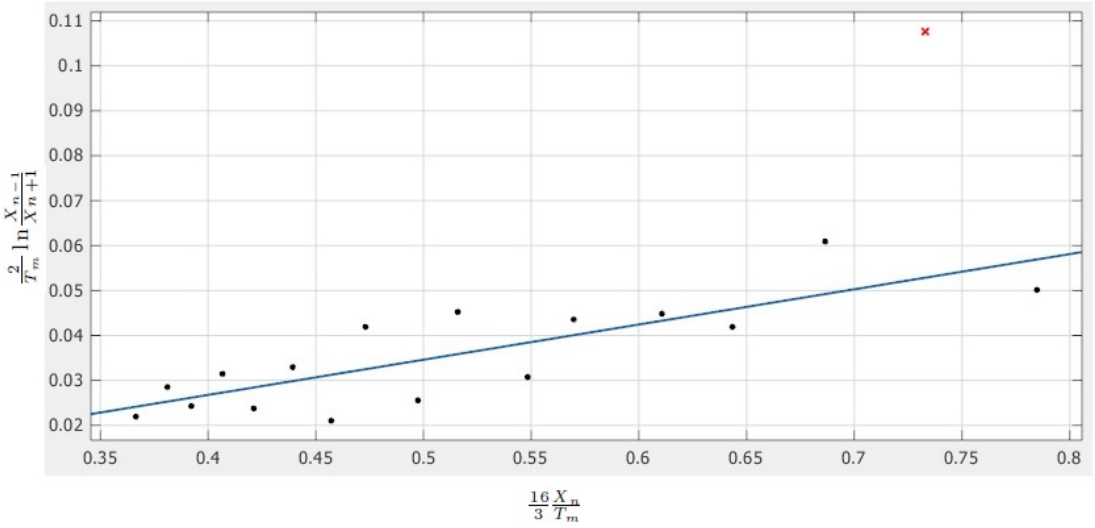

Figure 5.2: Step 4 after fitting a curve

The red cross on figure 5.2 represents values that were not taken into account.

5.4 Results

The most reliable way to obtain the roll damping of a ship at the present time seems to be to carry out model experiments, since the scale effect of damping is considered to be connected mainly with the skin friction of the hull, which makes a small contribution to total damping. The data from model testing can easily be transferred to the actual ship case by using an appropriate non-dimensional form of roll damping. The total roll damping for an ordinary hull can be divided into five components, that is, friction, eddy, lift and wave damping for bare hull and bilge keel damping.

$$B_e = B_F + B_E + B_L + B_W + B_{BK} \tag{5.5}$$

The term B_{BK} includes normal-force damping, hull-pressure damping and wave damping, all due to the bilge keels. Also other appendages can be included into the formula as for example the damping of a skeg that will be included in part 5.4.3 (skeg damping). Also other damping components can be neglected in the following decay experiments. The results of 4 different roll decay cases are listed in the subsequent subsections, including

a final parameter for p_1 and p_2, for each case. This parameter is calculated by the mean of all decay tests and will be used for further calculations.

5.4.1 Bare hull

As explained before, in total 4 different cases of roll decay tests are examined. Bare hull implies no propeller or other features that are attached on the hull. Therefore only the hull surface and form will give contribution to roll damping. One can focus on only 3 different damping contributions:

- radiated waves (not dominating in roll)
- turbulent skin friction between hull and water
- vortex shedding (eddy)

The wave damping B_W denotes the increment of the hull-pressure damping, due to the presence of free surface waves. It includes the interaction between waves and eddies and waves and lift. These interaction however are very small and one can assume them to be almost linear. The skin friction between hull and water is dominated by the model/ship material of the hull which gives a certain resistance that damps the roll motion. The friction damping is caused by the skin friction stress on the hull in roll motion. It may possibly be influenced by the presence of waves.

Decay Nr.	p_1	p_2
Decay 1	−0.003885	0.07834
Decay 2	−0.005550	0.08020
Decay 3	−0.002235	0.07125
Decay 4	−0.002505	0.07197
Decay 5	−0.006294	0.07999
Decay 6	−0.005682	0.07830
Decay 7	−0.006258	0.07910
Mean	**-0.004630**	**0.07702**

Table 5.1: Coefficients p_1 and p_2 calculated for each decay (bare hull)

The vortex damping (eddy damping) is caused by the pressure variation of the bare hull, excluding the effect of waves and bilge keels. It stands for the non-linear damping $p_2\dot{x}\,|\dot{x}|$. The form of the hull is a relevant factor for this damping.

5.4.2 Bilge keels

In order to increase the roll damping, passive stability systems such as bilge keels can be added to the hull. These appendages are usually constructed from flat plates that form a sharp obstruction to the roll motion (see fig 5.3). In order to have a minimal resistance while the ship is moving, the bilge keels are aligned with the calm water flow.

To aid this placement, one usually uses flow visualization. The length of the bilge keels is regularly selected to be such that the tip of the bilge keel lies within the maximum beam of the ship and above the baseline. By doing so, the ship's hull protects the bilge keel during docking, dry-docking and in shallow water. Bilge keels significantly improve

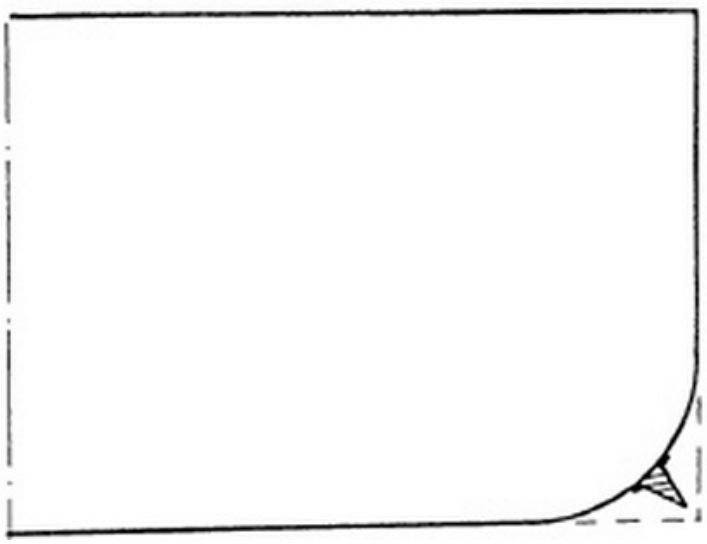

Figure 5.3: Typical bilge keel arrangement

the roll damping over that of a bare ship hull, but are less effective than what can be obtained by other roll stabilization devices. Still in most cases it is recommendable for a naval architect to install them, even when other stabilizers are fitted, thus only bilge keels are effective in the severest of seas. In addition to the damping components explained in

Decay Nr.	p_1	p_2
Decay 8	0.04624	0.3262
Decay 9	0.04669	0.3191
Decay 10	0.04500	0.3269
Decay 11	0.04611	0.3323
Decay 12	0.04098	0.3367
Decay 13	0.04075	0.3432
Decay 14	0.04300	0.3365
Mean	**0.04411**	**0.33156**

Table 5.2: Coefficients p_1 and p_2 calculated for each decay (bilge keel)

section 5.4.1 (bare hull), which are also present in this case, the bilge keel damping has to be introduced. It represents the increment of pressure damping due to the presence of a pair of bilge keels. This term consists of three components which are: The normal force damping of bilge keels, which is due to the normal force of the bilge keels itself. The

second component is the hull pressure damping due to bilge keels, which corresponds to the pressure change on the hull. One can regard this aspect as the interaction between hull and bilge keels. The rest is the wave damping of bilge keels, which is the interaction between the hull and the waves.

HIMENO [9] concludes that bilge keel damping is not merely a quadratic non-linear form, but that it depends on the roll amplitude and frequency in a more complicated manner. Furthermore, the effect of forward speed is not very large.

5.4.3 Skeg

Skegs are used to improve the maneuverability of the ship. In addition it upgrades the propulsion by concentrating the flow around the propeller disc. One can say that a skeg is a sternward extension of the keel of ships which have a rudder mounted behind. Vessel containing two rudders can therefore have twin skegs. Also multiple skegs are possible. Regarding the roll damping, one can say that from the physical point of view a skeg is

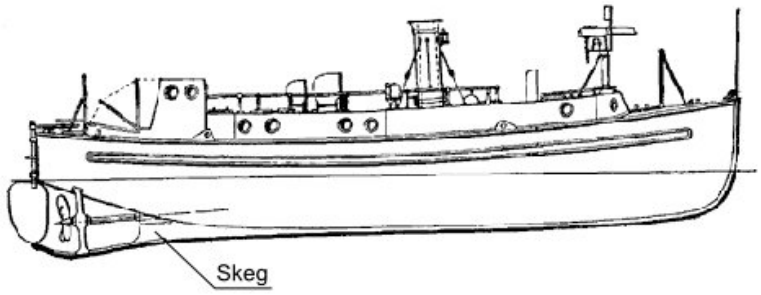

Figure 5.4: An example of a skeg arrangement

very similar to a bilge keel. It works likewise a bilge keel, containing the same damping characteristics.

Decay Nr.	p_1	p_2
Decay 15	−0.00444	0.1406
Decay 16	−0.02286	0.1773
Decay 17	−0.00950	0.1580
Decay 18	−0.03950	0.2106
Decay 19	−0.01028	0.1656
Decay 20	−0.03450	0.1822
Decay 21	−0.02300	0.1776
Mean	**-0.01915**	**0.17313**

Table 5.3: Coefficients p_1 and p_2 calculated for each decay (skeg)

One has to remember that the purpose of a skeg is not to damp the roll motion, in contrary to bilge keels. Still it contributes to roll damping, to what extent will be shown

later in section 5.6 (Analysis).

5.4.4 Combination

In this series of decay test the model contains bilge keels as well as a skeg. Both damping characteristics were explained in the sections 5.4.2 and 5.4.3. Basically one can say that both damping contributions are added together, as if an additional bilge keel would be added on. The roll damping is higher for the combination of both appendages (bilge keels and skeg), than either of them alone.

Decay Nr.	p_1	p_2
Decay 22	0.03006	0.3732
Decay 23	0.03100	0.3545
Decay 24	0.02800	0.3851
Decay 25	0.02865	0.3669
Decay 26	0.02901	0.3712
Decay 27	0.02820	0.3796
Decay 28	0.02831	0.3858
Mean	**0.02880**	**0.37376**

Table 5.4: Coefficients p_1 and p_2 calculated for each decay (bilge keel and skeg)

5.5 Neglecting the quadratic term

If non-linear terms, such as the p_2 coefficient, are not suitable for the calculations, then one can neglect the quadratic term and replace both coefficients (p_1 and p_2) into one equivalent damping term. By doing so, equation 5.3 becomes

$$\ddot{x} + p_{eq}\dot{x} + p_3 x = 0 \tag{5.6}$$

Here it should be noted that the equivalent damping coefficient p_{eq} does not replace the damping term p_1 that was calculated previously. However the energy loss per cycle (in the decay) for both, linear and quadratic term, should be equal to the equivalent coefficient. The calculation procedure to obtain p_{eq} is as follows. Find the damping ratio from the decay data assuming:

$$\xi = \frac{1}{2\pi} log(\frac{X_{n-1}}{X_{n+1}}) \tag{5.7}$$

Here X_{n-1} and X_{i+1} are considered to be two succeeding amplitudes. Knowing the natural roll amplitude of the ship, one can easily calculate p_{eq}:

$$p_{eq} = 2\omega_0 \xi \tag{5.8}$$

	Bare hull	**Bilge keel**	**Skeg**	**Combination**
p_{eq}	0.0412	0.101	0.0533	0.113
ξ	0.009	0.0227	0.0124	0.0268
$T[s]$	2.7473	2.809	2.9245	2.9716
$\omega[1/s]$	2.2870	2.2368	2.1485	2.1144

Table 5.5: Equivalent damping coefficients

Logically these values change, considering a bare hull or a ship with bilge keels and/or a skeg. Table 5.5 shows the equivalent damping coefficients for the decay tests mentioned earlier in section 5.4.

One can now compare the equivalent damping term with the linear and non-linear damping term. As mentioned before, both terms should damp the same amount of energy per cycle. For this reason, the code is run for both damping terms and the wave incident wave properties are kept the same. In a similar way, this has already been done

Wave frequency ω	7.9956 1/s
Wave amplitude ζ_a	0.015 m
Wave steepness k	0.0015 m

Table 5.6: Standard values for computation

in the project thesis. Comparing the angular displacement from the roll motion, one can see from the maximum obtained after the transient effect that both values nearly coincide. While using the linear and quadratic damping term the maximum is reached earlier than using the equivalent term. This means less incident wave periods are needed to reach the parametric roll resonance. The differences in the transient phase can be explained that the instability occurrence is more sensitive to the involved non-linearities and the approximations in the solver can be more restrictive. The simulations with the quadratic term and therefore the viscous damping corrections, should be more consistent with the experimental, physical results.

5.6 Analysis

The analysis is carried out with the 6DoF numerical solver, based on potential flow assumptions, presented in chapter 4. In order to work with the numerical solver one has to use a Unix-like operating system such as the *XFree86* software. Through this platform one can get access to the SSH channel, where the numerical solver is implemented. For the analysis, the incident wave properties and all other values are kept the same. The wave properties are listed in table 5.6. No more than the damping coefficients are changed, in order to visualize the sensitivity. For this reason, the linear and quadratic damping coefficients calculated in section 5.4 are scaled and transferred into the numerical algorithm. Here one has to distinguish between linear and quadratic term, as well as axial

and rotational displacement. Using the equation of motion for a ship, one can find the differences in the units. The linear damping term is proportional to the velocity, which gives a difference to the acceleration of $1/s$. Assuming Froude scaling is applied and a geometrical similarity with scale ratio $\lambda = L_F/L_M$ from the equality in time, one gets the relation

$$t_F = \sqrt{\lambda} t_M \tag{5.9}$$

As a consequence one gets

$$p_{1,F} = \frac{1}{\sqrt{\lambda}} p_{1,M} \tag{5.10}$$

The quadratic rotational damping term is dimensionless. Therefore one can assume

$$p_{2,F} = p_{2,M} \qquad (\text{for } \eta_4,\ \eta_5,\ \eta_6) \tag{5.11}$$

Finally one can obtain the coefficients that will be implemented in the numerical solver. The model size from the physical experiments is Lpp= 2.95m. Scaling to a length of 1m, one gets the following results (see table 5.7)

	Bare hull	**Bilge keel**	**Skeg**	**Combination**
p_1	-0.004630	0.04411	-0.01915	0.02880
$p_{1-scaled-to-1m}$	-0.007952	0.07576	-0.0329	0.04947
p_2	0.07702	0.33156	0.17313	0.37376

Table 5.7: Equivalent damping coefficients

5.6.1 Using equivalent damping coefficients

The results from table 5.5 are now implemented into the code. Only the damping coefficient is used instead of the linear and quadratic term. However, as mentioned before, the energy damped per decay cycle is equal in both approaches. It is of importance to compare the different damping parameters which automatically represent different hulls with or without appendages. Two main characteristics are compared here: the steady state roll amplitude while parametric rolling and the transient phase including the needed amount of waves for parametric roll occurrence. The latter is better described by the second approach using a quadratic damping term. Consequently the equivalent term is used for analyzing the steady state amplitudes. The importance lies within the maximum amplitude in the steady state condition. From table 5.5 one can already see the damping variable and expect the highest amplitudes with the smallest number of incident wasves. Smaller damping $\rightarrow$ less motions. In order to visualize the difference, one can take a look into the amplitudes in roll. Figure 5.5 shows the heave, roll and pitch amplitude of the bare hull. From this figure one can see the steady state roll motion with its maximum roll amplitude of 16.283 deg is reached after merely 290 wave crests. Furthermore, one

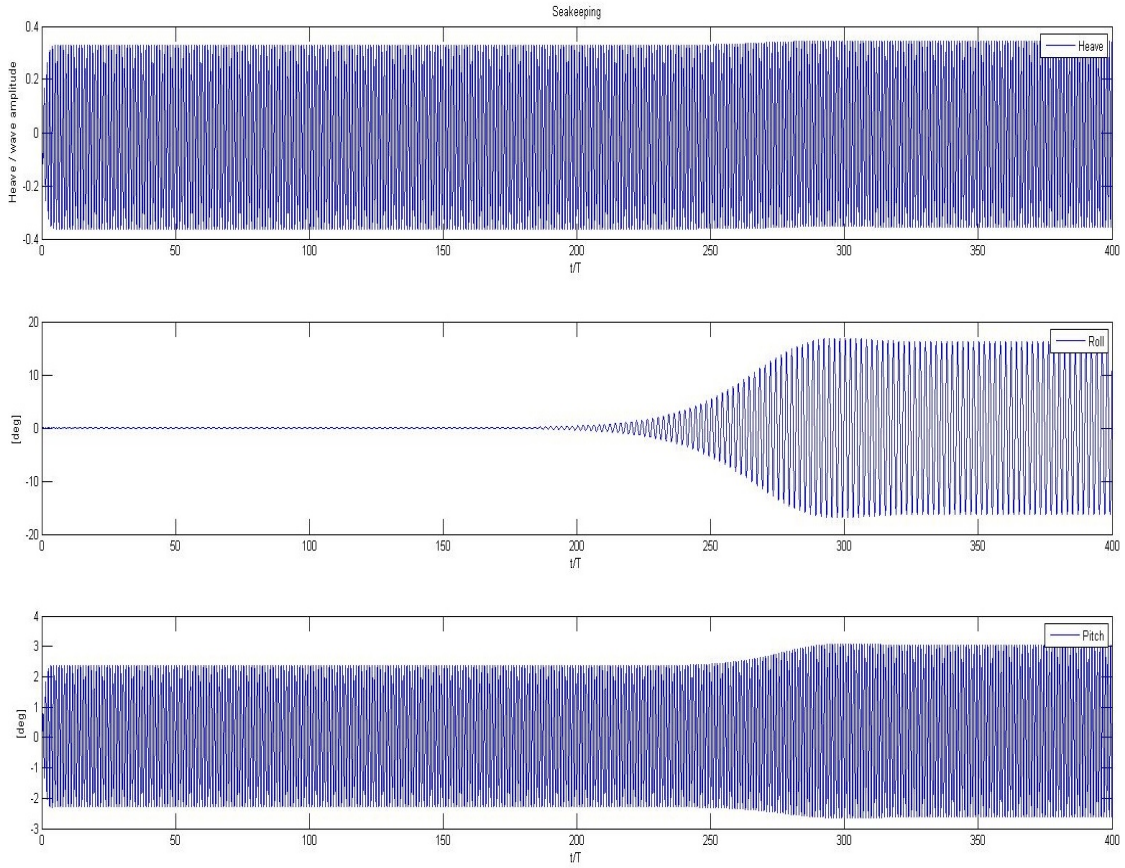

Figure 5.5: Seakeeping motions with a bare hull using the equivalent damping coefficient

can observe an interaction between the roll and pitch motion. Relative to the parametric roll motion of the same vessel with bilge keels, one can observe a drastic change in roll motion. Nearly no roll motion occurs. However the pitch motion as well as heave remain nearly equal. Concerning the maximum steady state roll amplitude with bilge keels, which occurs after around 420 incident wave crests, one has a magnitude of ≈ 2 deg.

To sum up, the roll amplitude while the ship is parametric rolling is as expected in the following order, starting with the highest amplitudes:

1. Bare hull
2. Skeg
3. Bilge keel
4. Combination of bilge Keel and skeg

Table 5.8 gives an overview of the roll amplitudes at steady state condition.

Bare hull	**Bilge keel**	**Skeg**	**Combination**
16.283 deg	$\approx$ 5 deg	15.41 deg	$\approx$ 4 deg

Table 5.8: Roll amplitudes using different appendages (equivalent linear damping coefficient)

From this results one can see the effect of a bilge keel or skeg relative to the roll amplitude. An enormous roll damping is achieved in attaching bilge keels to the hull. If however only a skeg is attached, then a small change in roll amplitude is recognizable. Using both together achieves the smallest amplitudes. Parametric rolling occurs, however the amplitude is so low that it is almost not noticeable.

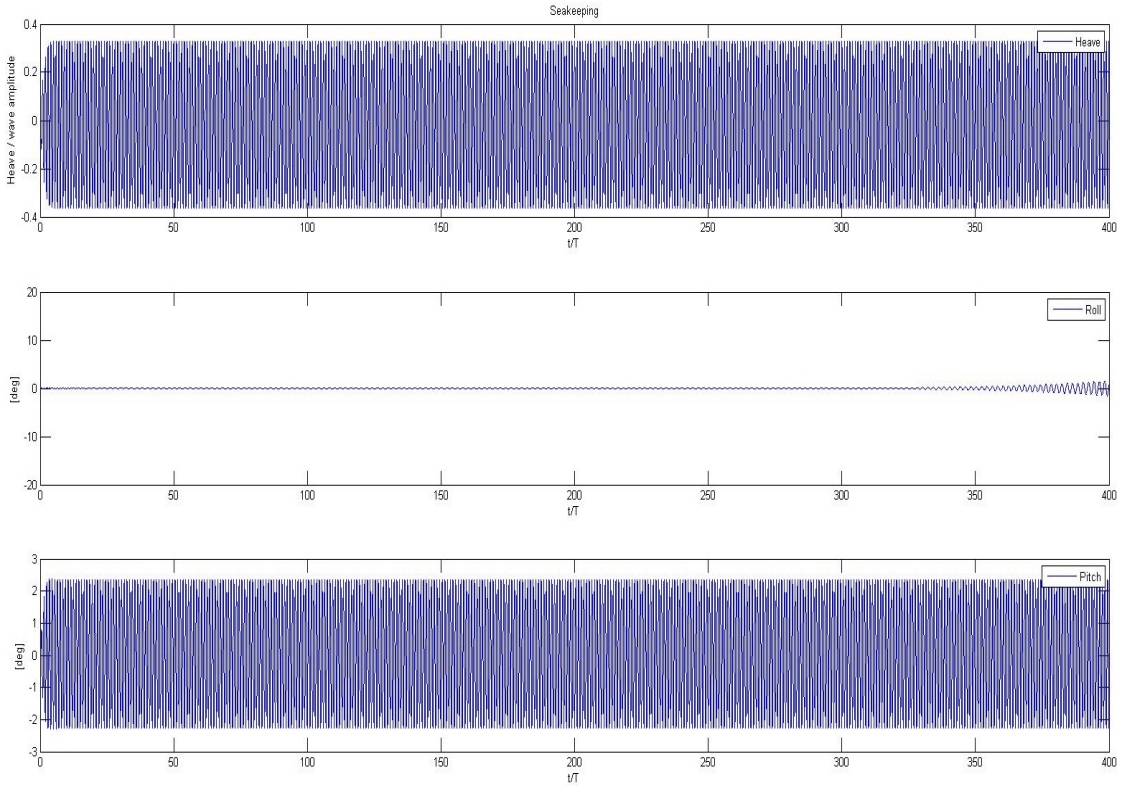

Figure 5.6: Seakeeping motions with a skeg attached to the bare hull using the equivalent damping coefficient

5.6.2 Using linear and quadratic damping

In this section the linear and quadratic damping coefficients are used instead of the equivalent damping term. The values are shown in table 5.7. In general, the results should

be more consistent with the experimental, physical results. The simulations with the quadratic term imply corrections for the viscous damping. In the former case only the wave-radiation roll damping from the linear potential-flow solver is modeled.

Two analysis are done here:

- comparison of the maximum amplitude (with the equivalent damping coefficients)
- analysis of the transient phase

Similar as in the previous section, the maximum roll angles while parametric rolling of the ship are determined. Results are shown in table 5.9. Basically one can observe that all maximum amplitudes are close to the previously obtained. A trend of slightly greater amplitudes can be observed. On the other hand, it is noticeable that the effect of a skeg is bigger. Being the difference for the equivalent damping coefficient between bare hull and skeg almost negligible, one can observe a considerable additional damping using a skeg with the quadratic damping term. The amplitudes using both, skeg and bilge keels, are higher than the results obtained from previous computations (difference of approximate 1 deg). It must be noted that only 400 incident wave periods were used for the calculations. In order to find the exact value for the steady state amplitude for bilge keels, one should increase the number of incident waves.

As a next step, the required amount of incident wave periods for parametric roll to occur is analyzed. The transient phase between the different models varies. Not only the time needed to reach parametric roll is different, but also the transient phase duration differs. In order to compare the various hull properties and its damping characteristics, the needed incident wave periods to obtain a roll motion of 1 degree is to be determined. Figure 5.7 shows the roll motion of the ship with additional bilge keels and a skeg. The vertical line at the incident wave period of 231 represents the reached roll motion angle of 1 deg.

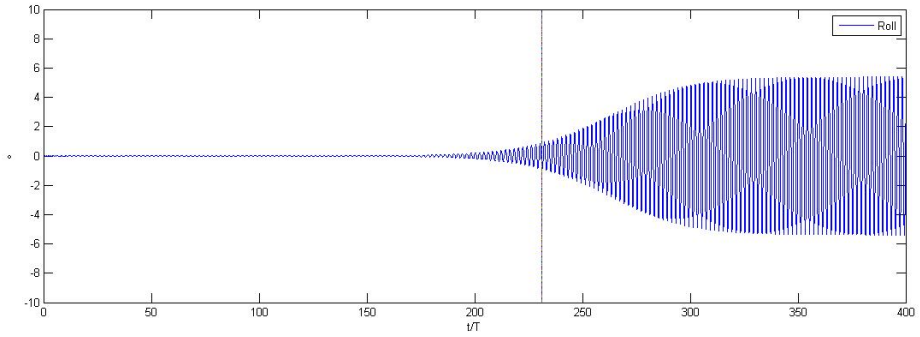

Figure 5.7: Roll motion for the hull with a combination of skeg and bilge keels

To sum up, the amplitudes while parametric roll occurrence (steady state condition) have an expected trend. The highest motions are found with the bare hull, followed by

skeg, bilge keels and finally the combination of both. This has already been shown using an equivalent damping term. Regarding the occurrence of parametric roll motion, one can observe that it starts the earliest (the smallest amount of incident wave periods) with a bare hull. However, comparing the bilge keels with the combination, one can see that it takes less incident wave periods for the combination (231 periods) than only bilge keels (294 periods). This can be explained, by the fact that the instability occurrence using bilge keels is more sensitive to the involved nonlinearities. Nevertheless, the main importance lies in the roll amplitudes which show the smallest motion in the combination using bilge keels and skeg.

	Bare hull	**Bilge keel**	**Skeg**	**Combination**
Amplitude	18.68 deg	≈ 6	13.08 deg	5.384 deg
Number of wave periods	113	294	138	231

Table 5.9: Roll amplitudes using different appendages (linear and quadratic damping coefficient) and number of wave periods to reach a roll angle of 1 deg

6 Investigation of parametric roll occurrence using a 1.5 DoF model

The analytical model introduced in chapter 3 has been implemented into MatLab for the analysis of parametric roll motion. As explained before, it is valid for longitudinal regular waves.

6.1 Procedure

There are many different approaches to analyze the parametric roll occurrence and its characteristics. Many coefficients can be modified and therefore a high number of different cases can be studied. However, in order to have comparable results, one should focus on certain parameters and keep other coefficients equal. In general, one can define an example of a numerical implementation with the following procedure:

1. Estimation of natural frequency and mechanical characteristics of the ship.
2. Define the damping parameters for the given case.
3. Select a particular wavelength and waveheight.
4. Calculate the restoring arm surface in waves using the analytical model (implemented in MatLab)
5. Fitting of the analytical $\overline{GZ}$ surface, to obtain the $Q_{jn}^{::}$ coefficients.
6. Select the ship speed range which is analyzed close to the first parametric roll resonance region.
7. Plot the results, showing the occurrence of parametric roll, position on the Ince-Strutt diagram and relative roll velocity and motion in time.

This procedure will be passed through several times, while some parameters are changed. The occurrence of parametric roll, including the roll velocity and amplitude are checked. Two major cases are studied separately: the ship as a bare hull and with a skeg.

6.2 Bare Hull

The characteristics of a ship with bare hull i.e. no bilge keel or other appendages, are already explained in chapter 5.4.1. From the model experiments one can extract

some parameters, as for example the natural roll frequency in calm water. In order to implement this coefficient in the 1.5 DoF model one has to scale the model natural roll frequency into a full scale ship frequency. The full scale to model scale is given as

$$\lambda = \frac{L_f}{L_m} = 10 \tag{6.1}$$

with a given natural roll frequency of $\omega_0 = 2.2870$ for the bare hull ship model (see table 5.5), the full scale natural roll frequency is calculated as

$$\omega_0 = 2.2870 \rightarrow f_{sc} = \frac{1}{s} = \frac{1}{\sqrt{\lambda}} = \frac{1}{\sqrt{10}} = 0.31623 \tag{6.2}$$

$$\omega_0 f_{sc} = 2.287 * 0.31623 = 0.7232[\frac{1}{s}] \tag{6.3}$$

For the bare hull this value will always be the same, as well as the mechanical characteristics of the ship. For simplicity, the damping parameter is set as $\mu = 0.05$. This starting value for the damping parameter is chosen, regarding realistic values for the given case. The influence of the damping parameter will be analyzed later on. In the next step the occurrence of parametric roll is analyzed as a function of the incident wave.

6.2.1 Case 1 – Changing the wavelength L_w

In this case the wave characteristics are chosen randomly. A waveheight of 2 meters is kept equal for all further calculations. However, the wavelength is changed and the related occurrence of parametric roll is analyzed. For better understanding, the wavelength is chosen as s function of the ship length i.e.

$$F(Lpp) = L_w \tag{6.4}$$

where Lpp denotes the ship length between perpendiculars and L_w the incident wave length. Table 6.1 shows the values which were used in the 1.5 DoF model.

Wavelength	**Velocity**	**Roll motion**	**Occurrence**
0.5 Lpp	0.065	0.013	X
0.7 Lpp	0.07	0.015	X
0.8 Lpp	0.44	0.1	$\surd$
0.9 Lpp	3.58	0.91	$\surd$
1 Lpp	0.87	0.21	$\surd$
1.1 Lpp	0.088	0.021	$\sim$X
1.2 Lpp	0.076	0.0185	X
1.3 Lpp	0.073	0.017	X
1.5 Lpp	0.071	0.0168	X

Table 6.1: Occurence of parametric roll for waveheight 2m and different wavelengths

As a next step the maximum roll motion is determined by finding the optimal wavelength that gives the highest parametric roll motion. For this reason one can take a look into the theory of the Mathieu diagram. With the relation

$$\sqrt{p} = \frac{\omega_0}{\omega_e} = 0.5 \tag{6.5}$$

one can determine the encounter frequency, which due to zero forward speed of the ship is equal to the wave frequency. In order to find the requested wave length the following formula can be used

$$L_w = \frac{2\pi g}{\omega_w^2} \tag{6.6}$$

This gives the wave properties for the largest parametric roll excitations. If the values

Wavefrequency $[\frac{1}{s}]$	**Wavelength [m]**	**Relative** L_w	**Roll motion**	**Occurrence**
1.4465	29.44	0.919945 Lpp	0.92	$\surd$

Table 6.2: Wave properties for $\frac{\omega_0}{\omega_e} = 0.5$

p and q for the above mentioned incident wave properties are plotted in the Mathieu diagram, one can see its position.

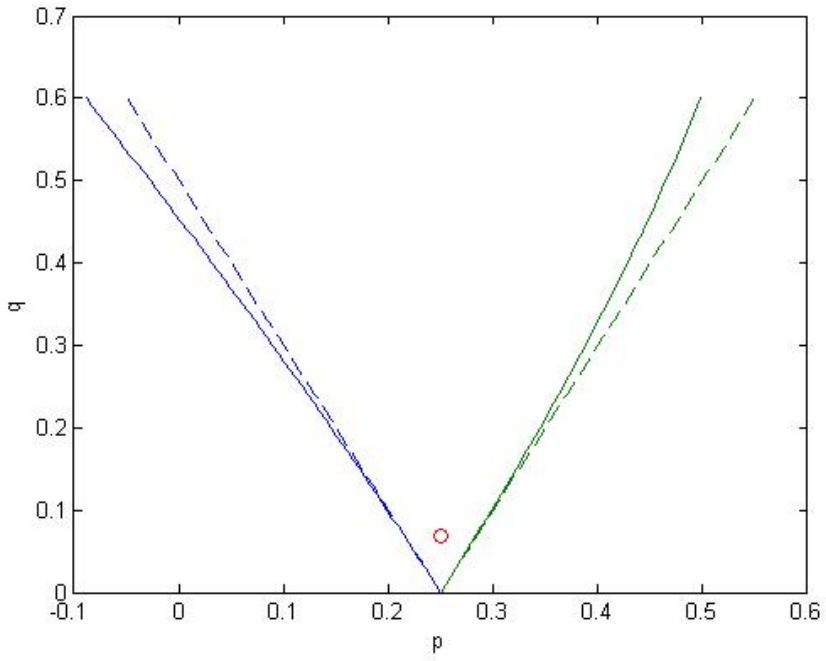

Figure 6.1: Mathieu diagram with p=0.2507 and q=0.0866

Taking the values from table 6.1 into the 1.5DoF model and solving the equations in time, one can compute the parametric roll motion. Starting with a roll angle of 1 deg, the amplitude of roll increases drastically. After 1 time step of 100 seconds, the ship encounters a roll angle of about 15.5 degrees. A critical angle of 45 degrees is already reached after 138 seconds. In theory capsizing of the ship could happen. Finally one

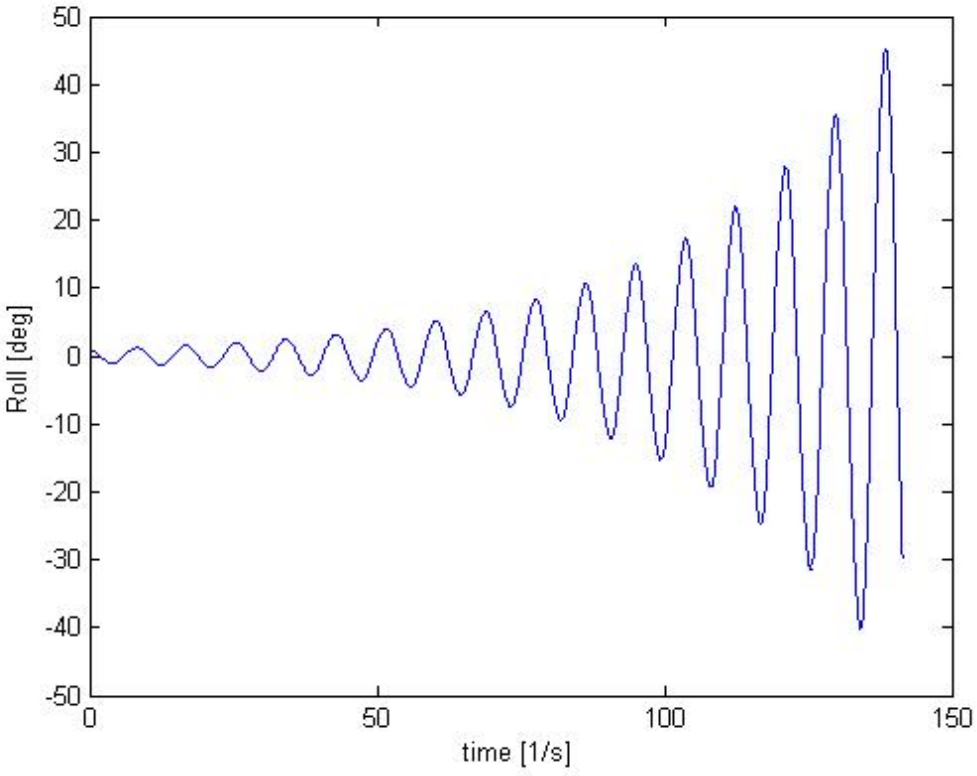

Figure 6.2: Roll motion in time for an incident wave of $H_w = 2m$ and $\omega_w = 1.4465$

can visualize the dependance of the wavelength H_w as a function of Lpp, relative to the parametric roll occurrence. The figure shows that the highest roll motion was found at a wavelength of $H_w \approx 0.92$Lpp. The straight line on figure 6.3 shows where the ship start with parametric rolling. It was found that a wavelength in between 0.74Lpp and 1.09Lpp leads to this phenomenon. All other wavelenghts i.e. underneath the straight line, will not give enough contribution to parametric rolling.

As a next step a closer look is taken into an edge case, where the parameters q and p lie on the borderline to a non-parametric roll case. For this reason, the wave from table 6.2 is taken into the 1.5DoF model and analyzed i.e. a wave with a wavelength of 1.1Lpp. On figure 6.4 one can see the given case where the red point (q=0.0905 and p=0.2998) lies beyond the line. From theory no parametric rolling should occur. This

is also the case and can be observed on the same figure (right). Although in the beginning the roll motion and velocity start to increase (from t=0 to t=18 seconds), they flatten out after a while. The roll motion and velocity go toward zero in a spiral pattern.

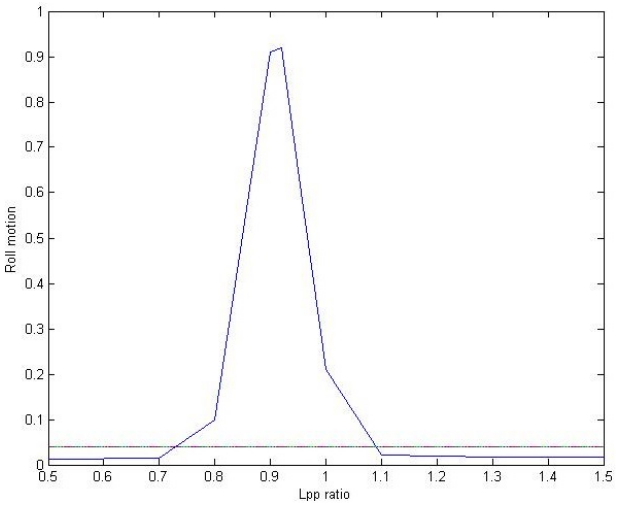

Figure 6.3: Roll motion vs wavelength

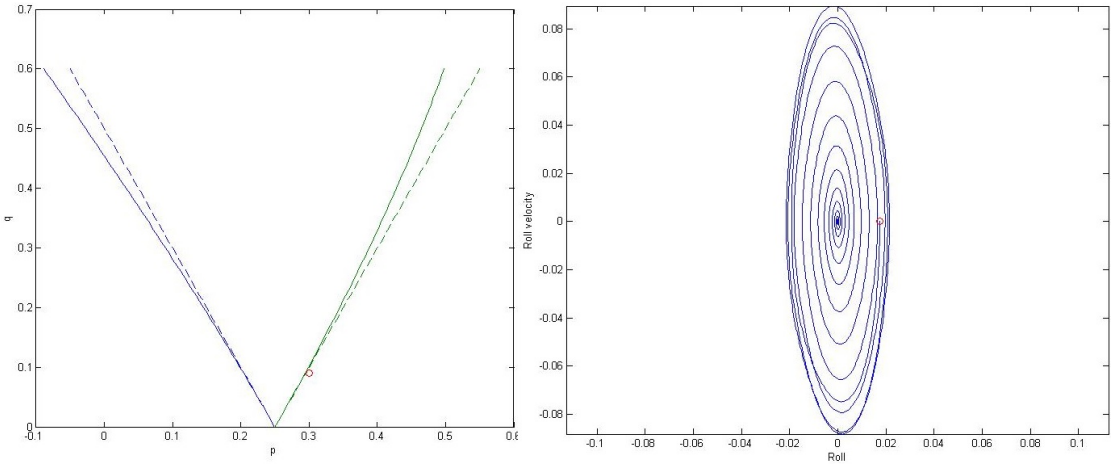

Figure 6.4: left - Mathieu diagram for edge case, right - progress of roll velocity and motion in time

6.2.2 Case 2 - Changing the waveheight H_w

After analyzing the wavelength as a function of Lpp, the incident waveheight is investigated. For this reason a wavelength is chosen and kept equal. Also the natural frequency

and mechanical characteristics of the ship, including the damping parameters, remain the same. As explained before the full scale natural roll frequency of the ship as a bare hull was previously calculated as $\omega_0 = 0.723\ [\frac{1}{s}]$. Using the relation $\sqrt{p} = \frac{\omega_0}{\omega_e} = 0.5$ an incident wave with a frequency is given as $\omega_w = 1.446[\frac{1}{s}]$. This yields to a wavelength of 29.44m which is an unchanged value in this case for further computations.

In case 1 the wavelength was constantly $H_w = 2$ meters. However in this case this parameter changes in order to see how the coefficients p and q alter. Also the occurrence of parametric roll is checked. Hence 15 new calculations were done with a variable waveheight, starting from $H_w = 0.25$ to $H_w = 5$ meters, using steps in between 0.25 and 0.5 meters.

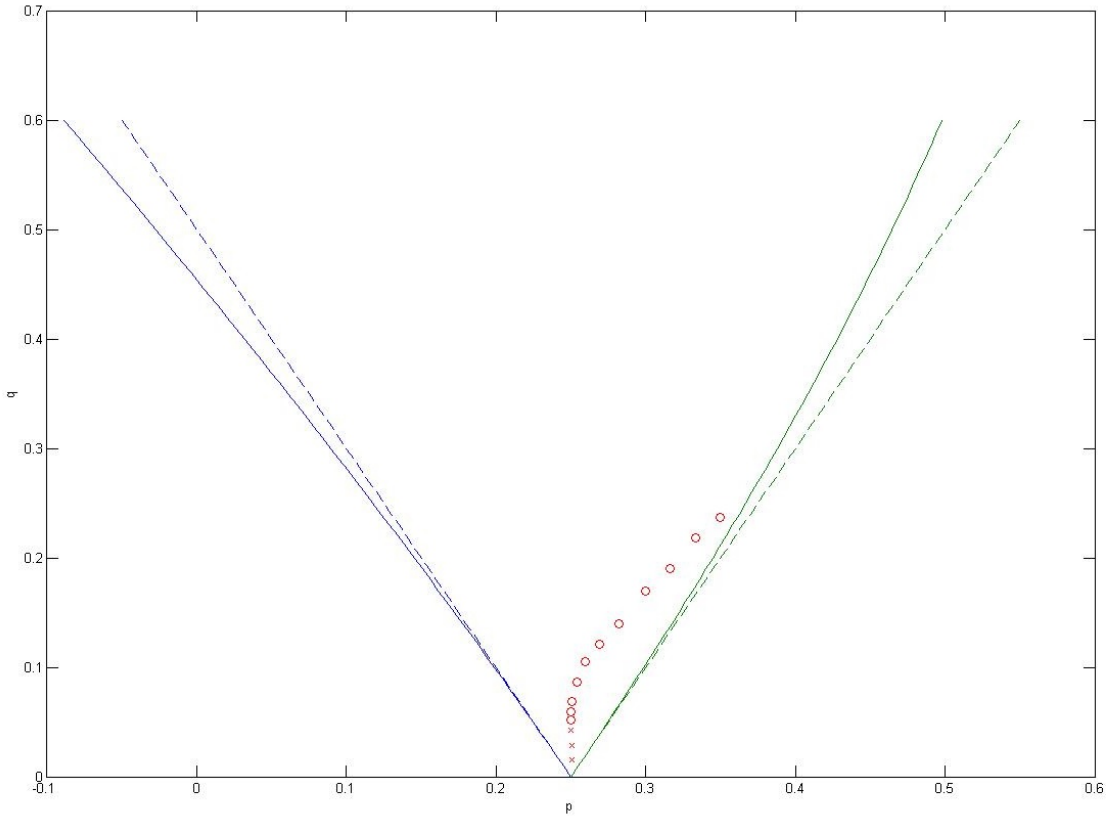

Figure 6.5: left - Mathieu diagram for edge case, right - progress of roll velocity and motion in time

The results are plotted on figure 6.5. Here one can see the instability region inside the wedge of the Mathieu diagram. The red circles and crosses represent the different

calculations with a varying waveheight where the values of p and q lie in between the instability boundaries. In theory all of these incident waves should excite the ship in a manner, so that parametric roll occurs. However the damping of the ship prevents a steady state parametric roll motion, when certain waves act on the body. These waves are marked with a red cross instead of a circle.

In summary it can be said that a greater waveheight will lead to a greater parametric roll motion. Also the transient phase to a steady state parametric roll motion should appear earlier. By increasing the damping characteristics of a ship a higher waveheight is needed to excite the ship, in order to reach a parametric roll occurrence.

Assuming a damping coefficient of $\mu = 0.05$, the edge case for parametric roll to occur was found for a waveheight of $H_w = 0.96$meters. It must be noted that this is only the case for a wave frequency of $\omega_w = 1.446[\frac{1}{s}]$. For this special case the roll motion does not flatten out after a time t, neither it increases. The roll motion and velocity given for time t=0 stay equal in infinity, as can be seen on figure 6.6. No transient phase emerges (see figure 6.7).

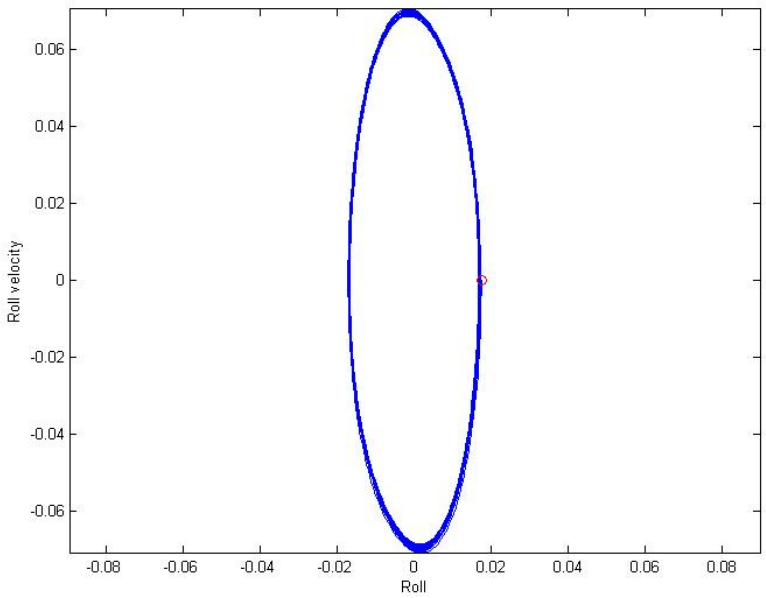

Figure 6.6: Roll motion and velocity for a waveheight $H_w = 0.96$m

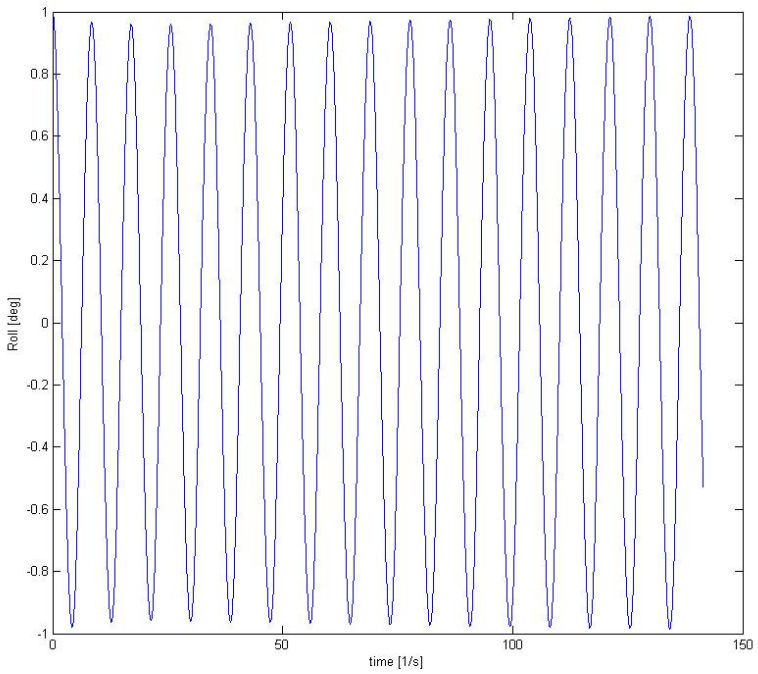

Figure 6.7: Roll motion in time for $H_w = 0.96$m - No transient phase

6.3 Fixed trim

As previously explained, one can analyze the ship stability using different approaches. An alternative way to examine the stability properties is to restrict the ship from having a trim. The so-called 'fixed-trim' calculations are compared with the free trim calculations obtained previously.

The initial static stability of the vessel (GM - metacentric height) is compared for both approaches. This is done as a function of the wave steepness. The following cases are evaluated:

	Wavelength λ_w[m]	**Waveheight** H_w[m]	**Wave steepness** $s_w = H_w/\lambda_w$	**Wave length ratio** λ_w/Lpp
Case 1	32	0.3200	1/100	1.000
Case 2	32	1.0667	1/30	1.000
Case 3	32	2.1333	1/15	1.000
Case 4	32	3.2000	1/10	1.000

Table 6.3: Numerical conditions for the metacentric height analysis

From all cases one can assess that the initial stability is higher for the 'fixed-trim' method, when the wave crest is at the ship FP and AP (front perpendicular, aft perpendicular). In particular, one can see from case 3 (figure 6.8) that the initial metacentric height is 1.0697m for 'fixed-trim' and 1.0097m for 'free-trim'. This is a difference of 6%. Furthermore it is important to notice the difference in the phase of the fluctuations between the two methods. This difference can be explained in the phase angle of the response as predicted by the analytical approach.

Concerning the minimum initial stability, one can observe that for case 3 both methods show an almost equal magnitude of the metacentric height (0.5217m for free-trim and 0.5286 for fixed-trim). Yet a difference where it occurs (wave crest position relative to Lpp) is notable. Being it amidships for 'free-trim' method, one can see that it is shifts 4.48m to the aftperperndicular for the 'fixed-trim'.

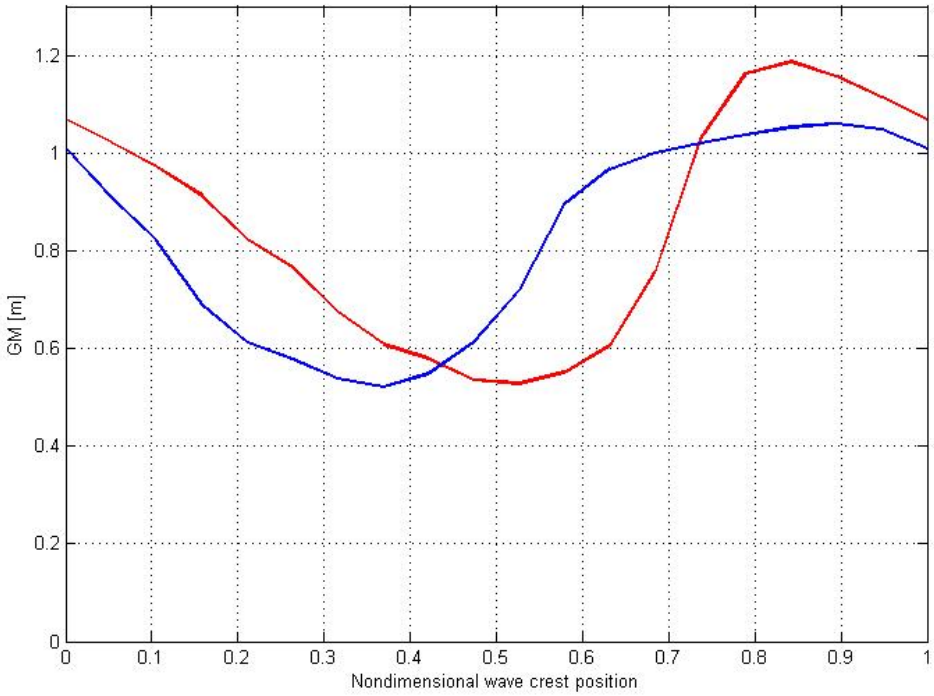

Figure 6.8: Calculated $\overline{GM}$ variation for case 3. Blue - free-trim; Red - fixed-trim

Comparing the results of the metacentric height with another model, one can see a similar trend. BULIAN (2006) predicted the metacentric height variation for a Destroyer CT1 with a ship length of Lpp= 126.6m. Generally, one can say that the 'fixed-trim' calculation is more conservative with respect to the 'free-trim' approach. Yet it is important to consider the requirements of the IMO intact stability code, which requires

static calculations using the 'free-trim' method. However this might be unsafe when considering quasi-static approaches.

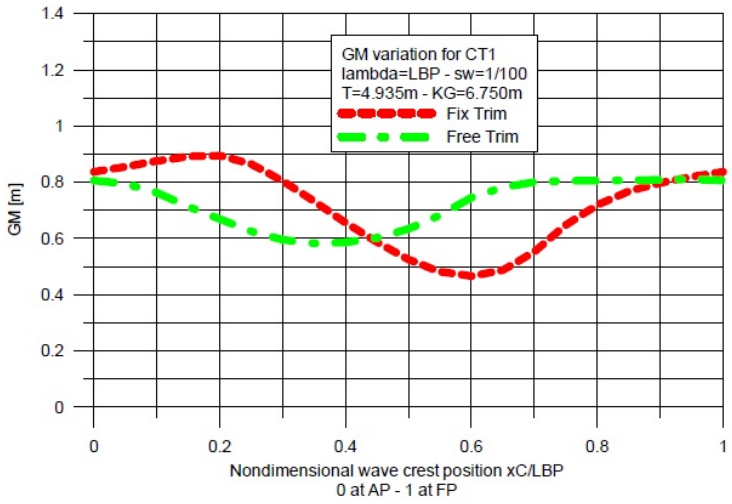

Figure 6.9: Calculated $\overline{GM}$ variation for CT1 - $\lambda_w/Lpp = 100$ and $s_w = 1/100$

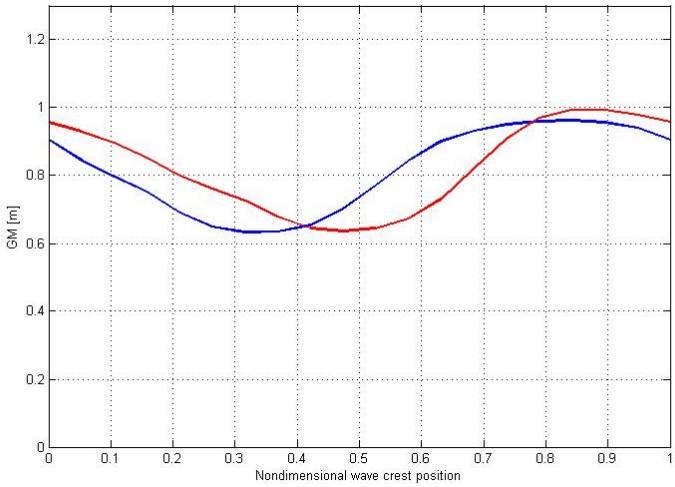

Figure 6.10: Calculated $\overline{GM}$ variation for case 2. Blue - Free-trim; Red - Fixed-trim

The results of case 1 and 4 can be found in Appendix B.

6.4 Skeg

For the same model which is used in the previous computation, an additional skeg is mounted. This new model is used as the input for further calculations in the 1.5DoF

model. Due to available experimental model testing data of the fishing vessel with a skeg, this section focuses on comparing the results of model testing with the 1.5DoF model. By doing so, one can determine the conformity of both methods.

The remaining input parameters for the 1.5DoF model were already determined in chapter 5, decay tests. The natural period of the vessel with skeg is T_n=2.94 sec, while the linear and quadratic damping coefficients are p_1=0.04411 and p_2=0.33156. These values were obtained from ship model decay tests and have to be scaled to a ratio of $\lambda = 1/10$.

In total 7 different edge cases will be calculated and compared afterwards with the experimental results.

	Natural Period T_n[s]	**Wave Period** T_w[s]	T_w/T_n	**Circular Wave steepness** kA
Case 1	9.234	4.710	0.51	0.1
Case 2	9.234	4.617	0.5	0.1
Case 3	9.234	4.432	0.48	0.1
Case 4	9.234	4.246	0.46	0.1
Case 5	9.234	4.710	0.51	0.15
Case 6	9.234	4.617	0.5	0.15
Case 7	9.234	4.432	0.48	0.15

Table 6.4: Input data for the 1.5DoF model

The results of the calculations are given in the next chapter (7, Experimental campaign) in order to analyze them with the models tests.

7 Experimental campaign

The experimental campaign took place in the ship model basin of the institute CNR - INSEAN situated in Rome, Italy. It was performed by Dr. Claudio Lugni. A parametric roll study of a fishing vessel model with the following characteristics was carried out:

Ship Info		
Length over all	LOA	33.99 m
Length between perpendiculars	Lpp	29.5 m
Beam overall	BOA	9.5 m
Depth overall	D	9.27 m
Volume displacement	∇	640.775 m^3
Waterplane area	A_w	253 m^2
Block coefficient	c_b	0.449

Table 7.1: Main particulars of the fishing vessel model

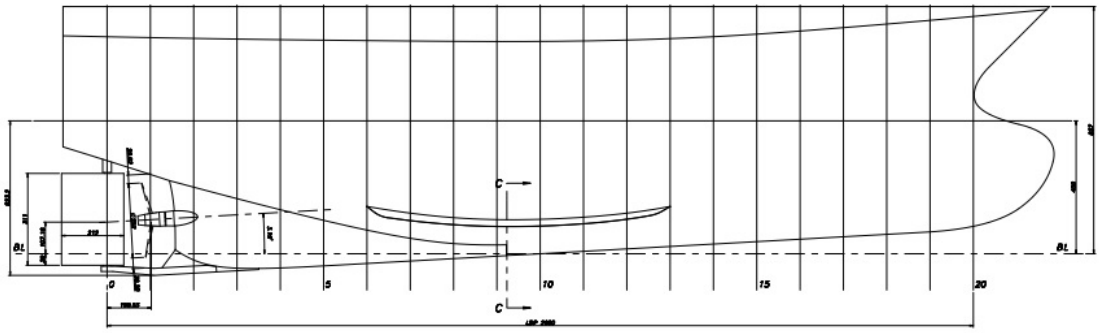

Figure 7.1: Body plan of the fishing vessel

Validation of a numerical code means to check if the computer program is consistent with the physical reality. For this purpose, model tests play an important role. From a selected data, the relevant tests were taken out, in order to compare them with the 1.5DoF model calculations. The results are shown in table 7.2.

	Natural Period T_n[s]	**Wave Period** T_w[s]	T_w/T_n	**Circular Wave steepness** kA	**Occurrence**
Case 1	2.92	1.49	0.51	0.1	√
Case 2	2.92	1.46	0.5	0.1	√
Case 3	2.92	1.40	0.48	0.1	X
Case 4	2.92	1.34	0.46	0.1	X
Case 5	2.92	1.49	0.51	0.15	√
Case 6	2.92	1.46	0.5	0.15	√
Case 7	2.92	1.40	0.48	0.15	√

Table 7.2: Input data for the test runs in the towing tank

7.1 Model test for validation of numerical calculations

The results obtained from the model tests (table 7.2) are compared with the results from the calculations from table 6.4. The cases that are analyzed are edge cases, where parametric roll motion might occur or not. Table 7.2 shows when parametric rolling occurs for the experiments. For the 1.5DoF model the input data was obtained from the experiments e.g. (natural period, table 6.4 and damping table 5.5) and scaled to the actual size. Then the results from section 6.4 are compared with the experiments.

By comparing both results from the experiments and numerical calculations, one can see that they coincide. Although the difference between the cases are rather small (small changes in incident wave lengths), they still agree with the experiments. This shows that the model is quite accurate. Finally one can confirm that the 1.5DoF model is consistent with the experimental results.

7.2 Uncertainties

In order to carry out a computer code validation using model test results, one needs to identify possible error sources, both for the model tests and for the numerical model. In principle an uncertainty analysis should be carried out. This means that possible error sources should be determined for the numerical analysis, as well as experimental results. The effect of each error source should be systematically investigated by numerical calculations. The validation procedure depends on the actual problem, in this case the sensitivity of parametric roll occurrence. The steps for a validation procedure are:

1. Equal model loading condition; Ensure that the model and numerical parameters are the same
    - Geometry (with or whiteout skeg)
    - Vessel draft and trim
    - Metacentric height

- Radius of gyration

2. Equal environment; Examine the environmental data used in model tests.
   - Wave height H and period T
   - Effect of water depth
   - Diffracted and reflected waves of the roll motion
3. Equal test condition; Ensure that model test and calculations are carried out for the same test cases
   - Forward speed
   - Wave heading
   - Transient effects
4. Natural periods and damping; Compare calculated and measured roll damping.
5. Influence of error ranges on results; Establish by numerical calculations the effect of error ranges for the different parameters (mainly roll damping) on the final results.
6. Comparison of results; The occurrence of parametric roll as well as the transient phases and the maximum roll angle.

8 Conclusions and Further work

8.1 Conclusions

The main focus of this study has been on parametric rolling and the aim was to analyze the sensitivity of parametric roll occurrence and features on a fishing vessel to the environmental conditions. To achieve this, a 6DoF potential flow solver was used to compare different damping characteristics, which are related to different hull models or appendages respectively. Furthermore, a 1.5DoF model was examined and used to investigate the occurrence of parametric roll while changing the environmental conditions. Lastly, experimental model tests were used to validate the 1.5DoF method.

From decay tests of the fishing vessel, the differences in damping were obtained. As expected the lowest damping was calculated from a bare hull. Adding a skeg to the model gives a small increase in roll damping. Concerning bilge keels, one can observe a considerable roll damping increase. The highest damping was found by the combination of skeg and bilge keels. Using the 6DoF potential flow solver, the maximum roll angle for a given incident wave (where parametric rolling occurs) was obtained. The steady state roll amplitude while parametric rolling was around 4 times smaller than using only the bare hull model. These calculations were done using equivalent damping coefficients as well as linear and quadratic terms. The latter simulations are more consistent with the physical results as they include viscous damping corrections.

For the 1.5DoF model the sensitivity of parametric roll occurrence was analyzed by changing the incident wavelength and waveheight. This has been done separately by keeping all values the same and using the wave properties as variables. Knowing the damping parameters, one can then easily find the critical incident wave length or height for parametric rolling to occur. The feature of using a fixed-trim or free-trim method, changes the initial stability and therefore also when parametric roll takes place, being the initial stability higher for the fix-trim method, when the wave crest is at the ship ends. However both methods follow a similar trend with a noticeable phase shift. Generally it can be said that the fixed-trim calculation is more conservative with respect to the free-trim approach.

The validation of the 1.5DoF model was done using experimental data from model tests which took place in the ship model basin of the institute CNR-INSEAN. By comparing edge cases where instability of the vessel occurs and nearly occurs, it could be showed that both the 1.5DoF numerical method and the experimental results coincide. It can be said that the 1.5DoF model is consistent with the physical experiments.

8.2 Further work

The occurrence of parametric rolling is largely dependent on the hull form and the encounter conditions. While the focus has been on a fishing vessel, other hull forms with different appendages or such as larger container vessels or smaller ships are not excluded from encountering this phenomenon. This study may be extended onto different hull forms in order to see how the codes (6DoF and 1.5DoF model) fares with them to widen its area of application.

The experimental results were only compared with the 1.5DoF model, however it could be of interest to verify also the physical model results with the 6DoF potential flow solver. By doing so, not only the occurrence could be checked but also if the maximum roll angle while parametric rolling is consistent with the experiments.

Considering that the 1.5DoF model does not include all 6 rigid ship body motions, it would be interesting to study to what extent other motions such as yaw are necessary for a reliable analysis of parametric roll. The coupling of other ship motions can have considerable effect on the ship stability and it is not considered in the 1.5DoF model.

Since bilge keels showed a considerable increase in roll damping, it would be of interest to study further cases by including them. This could be done experimentally, but also using the 1.5DoF model and comparing the occurrence with the results from the numerical 6DoF method.

9 Nomenclature

Symbol	Description
$\overline{BM}$	Metacentric radius
$\overline{GM}$	Transverse metacentric height
$\overline{GZ}$	Righting arm about center of gravity
$\overline{KB}$	Distance from keel to the vertical center of buoyancy
$\overline{KG}$	Distance from keel to the vertical center of gravity
A	Sectional area
A_w	Water plane area
A_{jk}	Added mass matrix component
B	Ship beam
B_{jk}	Damping matrix component
B_e	Total roll damping
B_E	Eddy damping
B_{BK}	Bilge keel damping
B_F	Friction damping
B_L	Lift damping
B_W	Wave damping
c_b	Block coefficient
C_d	Drag coefficient
C_m	Inertia coefficient
C_{jk}	Restoring matrix component
c_w	Wave celerity
D	Propeller diameter
E	Young's modulus
F_j^{FK}	Froude-Krilov force amplitude, for $j = 1..6$
F_n	Froude number
F	Force in general
F_g	Gravitational force
F_{rsc}	Radiated and scattering force
f_{sc}	Scale coefficient
G	Center of gravity
g	Gravitational constant
H_w	Waveheight

Symbol	Description
$H(\omega)$	Mechanical transfer function
i	Imaginary unit
I	Second moment of area
I_j	Moment of inertia
I_{jk}	Product of inertia
J	Advance coefficient
K	Keel
k	Wave number
Lpp	Length between perpendiculars
L_w	Wave length
L_f	Full scale ship length
L_m	Model scale ship length
m	Meters
M_{jk}	Mass matrix component
N_p	Polynomial fitting degree
n	Propeller rate of revolution
$Q_{jn}^{\cdot}$	Transformed Fourier coefficients
p	Pressure in general
p_{eq}	Equivalent damping term
p_1	Linear damping term
p_2	Quadratic damping term
Re	Reynolds number
S_w	Wetted surface
s_w	Wave steepness
t	Time
T_e	Period of encounter
T_e	Period of roll decay peak
V	Volume of the body
V_s	Ship speed
We	Weber number
x_c	Wave crest position along the hull
Greek symbols	
ϵ	Phase angle
η_j	Modes of rigid body motions
η_{Rj}	Real part of complex motion amplitudes
η_{Ij}	Imaginary part of complex motion amplitude
λ	Scale factor

Symbol	Description
ϕ	Static heel angle
ω_w	Wave frequency
ω_e	Encounter frequency
ω_0	Natural roll frequency
Ω	Angular velocity
ν	Kinematic viscosity
ϑ	Pitch angle
Φ	Velocity potential
ρ	Water density
χ	Angle between ship heading and wave propagation
ξ_i	Ship body motions along body the coordinate system
ξ	Damping ratio
ζ_a	Wave amplitude
Abbreviations	
BOA	Breadth Over All
DNV	Det Norske Veritas
DoF	Degrees of Freedom
IMO	International Maritime Organization
LOA	Length Over All
SSH	Secure Shell

Bibliography

[1] GRECO, M. AND C. LUGNI (2012). 3-D seakeeping analysis with water on deck and slamming. Part 1: numerical solver. In press on Journal of Fluids and Structures

[2] GRECO, M. AND C. LUGNI (2012). Numerical and experimental study of parametric roll with water on deck

[3] FALTINSEN, O.M. (1998). SEA LOADS ON SHIPS AND OFFSHORE STRUCTURES. Cambridge University Press

[4] STEEN, S. and AARSNES, J.V. (2001). TMR7 - Experimental Methods in Marine Hydrodynamics (Revised August 2012). Trondheim, Norway: Department of Marine Technology

[5] BULIAN, G. (2006). Development of analytical nonlinear models for parametric roll and hydrostatic restoring variations in regular and irregular waves

[6] RIBEIRO e SILVA, S., SANTOS, T.A., GUEDES SOARES (2010) - On the Parametric Rolling of Container Vessels

[7] T.M. AHMEDN, D.A.HUDSON,P.TEMAREL (2010) An investigation into parametric roll resonance in regular waves using a partly non-linear numerical model

[8] K.J. SPYROU, I. TIGKAS, G. SCANFERLA, N. THEMELIS(2007) -Prediction potential of the parametric rolling behavior of a post-panamax container ship

[9] HIMENO, YOJI (1981) - Prediction of ship roll damping - State of the art

[10] PARK, J.-H., TROESCH, A. W. Numerical modeling of short-time scale nonlinear water waves generated by large vertical motions of non-wallsided bodies. Proc. 19th Svmp. on Naval Hydrodynamics, Seoul, Korea, 199

[11] HANSELMAN, Duane and Bruce Littlefield. Mastering Matlab 5. (1998) New Jersey: Prentice Hall

[12] GEYSSEL, J (2013) Project thesis in Marine Technology - Experimental Study of Parametric Roll

[13] Massachusetts Institute of Technology, WAMIT *Version 5.1 - A Radiation-Diffraction Panel Program For Wave-Body Interactions*, Userguide, 1994

[14] GRAW, K.-U.; *Wellenenergie, eine hydromechanische Analyse*, Lehr- und Forschungsgebietes Wasserbau und Wasserwirtschaft, Bergische UniversitÃt - GH Wuppertal, 1995

[15] CLAUSS, G.,LEHMANN, E. OESTERGAARD, C.,*Meerestechnische Konstruktionen*, Springer Verlag Berlin Heidelberg New York (1988)

[16] CLAUSS, G.,LEHMANN, E. OESTERGAARD, C.,*Offshore Structures - Volume 1 - Conceptual Design and Hydromechanics*, Springer Verlag London (1992)

10 Appendix A

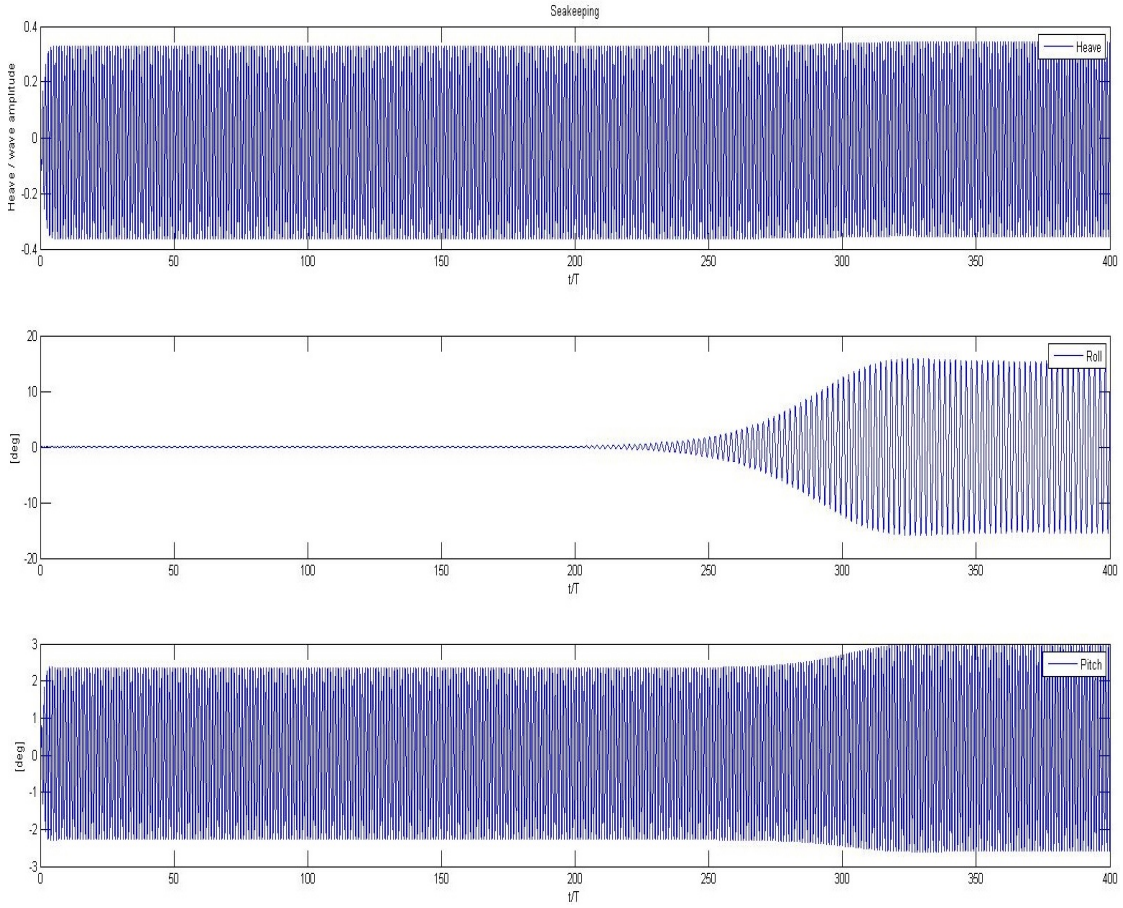

Figure 10.1: Seakeeping motions with a bilge keel attached to the bare hull using the equivalent damping coefficient

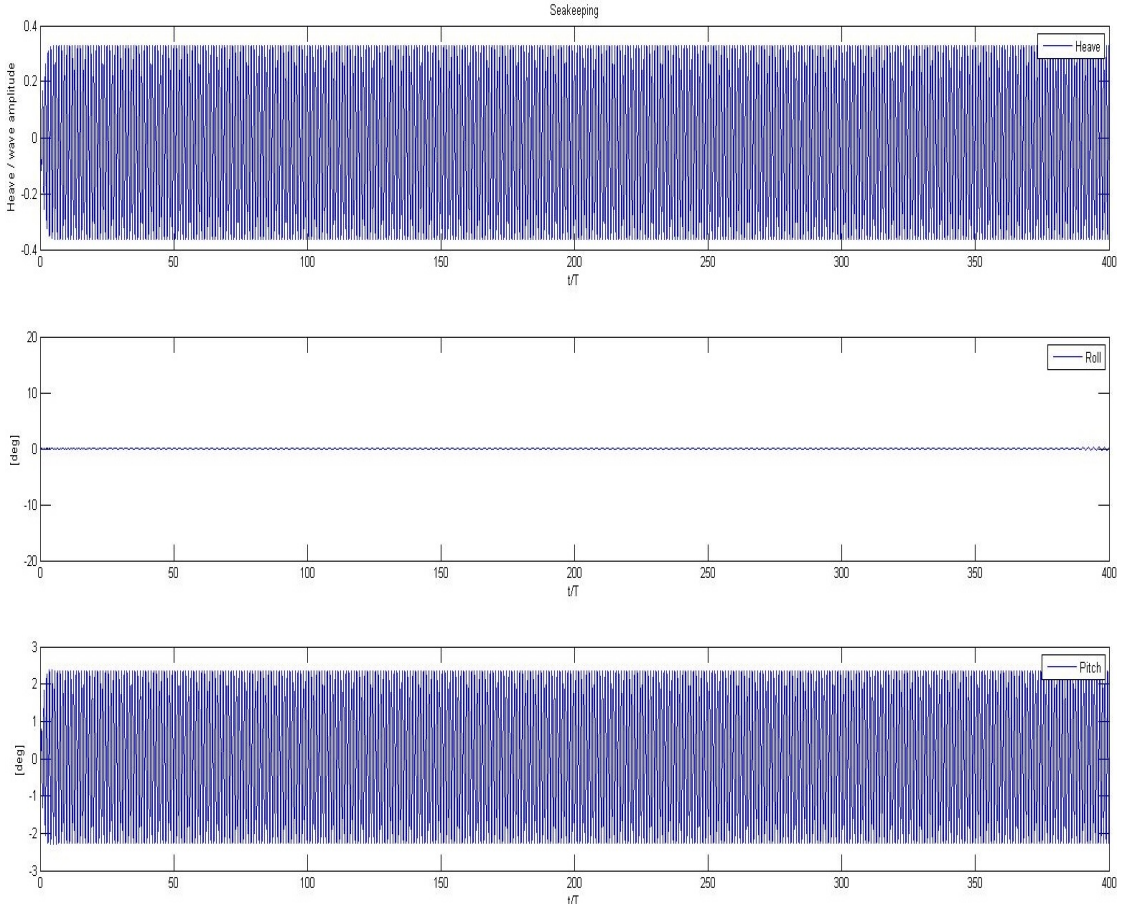

Figure 10.2: Seakeeping motions with a skeg and bilge keel attached to the bare hull using the equivalent damping coefficient

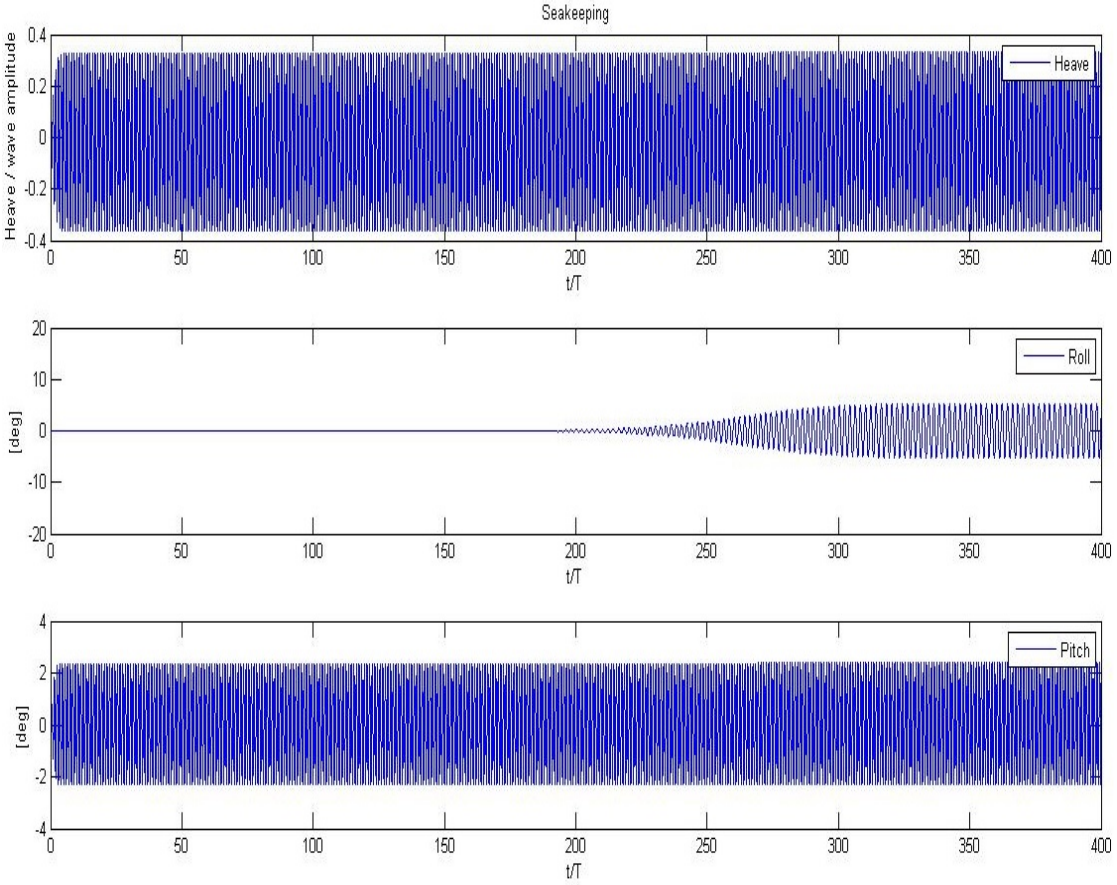

Figure 10.3: Seakeeping motions with a skeg and bilge keel attached to the bare hull using the linear and quadratic damping coefficient

11 Appendix B

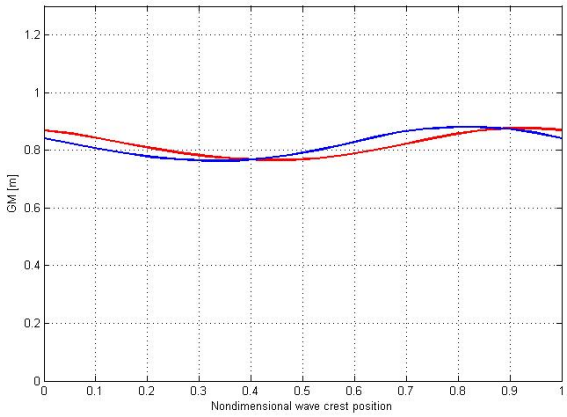

Figure 11.1: Calculated $\overline{GM}$ variation for case 1. Blue - Free-trim; Red - Fixed-trim

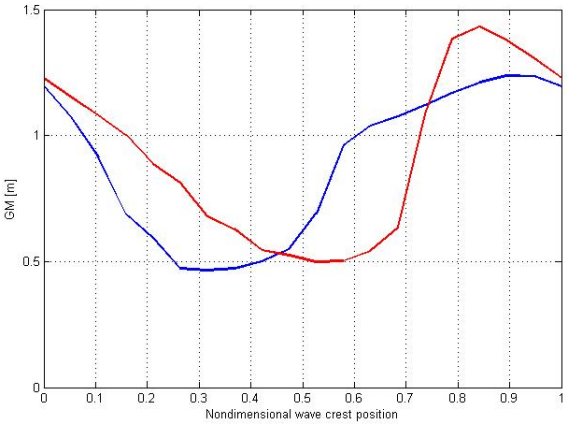

Figure 11.2: Calculated $\overline{GM}$ variation for case 4. Blue - Free-trim; Red - Fixed-trim

12 Appendix C

Here the MatLab codes used in this Master thesis are presented.

motions.m

```
clc
clear

mot = load('C:\Users\Johi\Desktop\roll\dsolnew.txt');
Time = mot(:,1);
surge = mot(:,2);
sway = mot(:,3);
heave = mot(:,4);
roll = mot(:,5);
pitch = mot(:,6);
yaw = mot(:,7);


 figure(1);
 plot(Time,roll);
 xlim([0 400]);
 ylim([-10 10]);
 hold on

 r=231
 e=[-10:0.01:10]
 plot (r,e)


 xlabel('t/T');
 ylabel('Â°');
 legend('Roll');

figure(2)
subplot(3,1,1)
plot(Time,surge);
xlim([0 400]);
xlabel('t/T');
```

```
ylabel('Surge / wave amplitude');
legend('Surge');
title('Manouevring')

subplot(3,1,2)
plot(Time,sway);
xlim([0 400]);
xlabel('t/T');
ylabel('Sway / wave amplitude');
legend('Sway');

subplot(3,1,3)
plot(Time,yaw);
xlim([0 400]);
xlabel('t/T');
ylabel('[deg]');
legend('Yaw');

figure(3)
subplot(3,1,1)
plot(Time,heave);
xlim([0 400]);
xlabel('t/T');
ylabel('Heave / wave amplitude');
legend('Heave');
title('Seakeeping')

subplot(3,1,2)
plot(Time,roll);
xlim([0 400]);
ylim([-20 20]);
xlabel('t/T');
ylabel('[deg]');
legend('Roll');

subplot(3,1,3)
plot(Time,pitch);
xlim([0 400]);
xlabel('t/T');
ylabel('[deg]');
legend('Pitch');
```

Natural frequency

```
figure(1);
[P1,F1] = pwelch(Angle,[],[],[],(1./0.0018));
plot(F1,P1);
xlim([0 1]);


xlabel('Frequency [s-1]');
ylabel('Spectral density');

[Y_1X,i_1X] = max(P1);
Oscillation_frequenzy = F1(i_1X)
```

Decay test

```
figure(1);
plot(Time,Angle);
xlabel('Time [s]');
ylabel('Roll angle [deg]');
legend('Decay (Roll)');

max(Angle);


for i= 1:1530;
     Decay1(i) = Angle(8+i,:);
end
max1=max(Decay1)*pi/180;
for i= 1:1530;
     Decay2(i) = Angle(1535+i,:);
end
max2=max(Decay2)*pi/180;
for i= 1:1530;
     Decay3(i) = Angle(4595+i,:);
end
max3=max(Decay3)*pi/180;
for i= 1:1530;
     Decay4(i) = Angle(6125+i,:);
end
max4=max(Decay4)*pi/180;
for i= 1:1530;
```

```
     Decay5(i) = Angle(7655+i,:);
end
max5=max(Decay5)*pi/180;
for i= 1:1530;
     Decay6(i) = Angle(9185+i,:);
end
max6=max(Decay6)*pi/180;
for i= 1:1530;
     Decay7(i) = Angle(10715+i,:);
end
max7=max(Decay7)*pi/180;
for i= 1:1530;
     Decay8(i) = Angle(12245+i,:);
end
max8=max(Decay8)*pi/180;

%%%%%%%%%%%%%%%%%%%%%%%%%%%%%%%%%%%%%%%%%%%%%%%%%%%%%%%%%%%%%%%%%%%%%%%

for i= 1:1530;
     Decay1(i) = Angle(775+i,:);
end
min1=min(Decay1)*pi/180;
for i= 1:1530;
     Decay2(i) = Angle(2305+i,:);
end
min2=min(Decay2)*pi/180;
for i= 1:1530;
     Decay3(i) = Angle(3835+i,:);
end
min3=min(Decay3)*pi/180;
for i= 1:1530;
     Decay4(i) = Angle(5365+i,:);
end
min4=min(Decay4)*pi/180;
for i= 1:1530;
     Decay5(i) = Angle(6895+i,:);
end
min5=min(Decay5)*pi/180;
for i= 1:1530;
     Decay6(i) = Angle(8425+i,:);
end
min6=min(Decay6)*pi/180;
for i= 1:1530;
     Decay7(i) = Angle(9955+i,:);
```

```
end
min7=min(Decay7)*pi/180;
for i= 1:1530;
     Decay8(i) = Angle(11485+i,:);
end
min8=min(Decay8)*pi/180;

osc.freq=0.373
T=2.7473

damp1=(log(max1/max2))*(2/T);
damp2=(log(max2/max3))*(2/T);
damp3=(log(max3/max4))*(2/T);
damp4=(log(max4/max5))*(2/T);
damp5=(log(max5/max6))*(2/T);
damp6=(log(max6/max7))*(2/T);
damp7=(log(max7/max8))*(2/T);
damp8=(log(max8/max9))*(2/T);


damp=[damp1,damp2,damp3, damp4, damp5, damp6, damp7, damp8]

right1=(16/3)*abs(min1/T);
right2=(16/3)*abs(min2/T);
right3=(16/3)*abs(min3/T);
right4=(16/3)*abs(min4/T);
right5=(16/3)*abs(min5/T);
right6=(16/3)*abs(min6/T);
right7=(16/3)*abs(min7/T);
right8=(16/3)*abs(min8/T);
right=[right1, right2, right3, right4, right5, right6, right7, right8]

figure(4)
plot(damp,right)
```